Gondwana Research 137 (2025) 145–170

Contents lists available at ScienceDirect

Gondwana Research

journal homepage: www.elsevier.com/locate/gr

The mid-Cretaceous bauxites of SE France: Geochemistry, U-Pb zircon dating and their implications for the paleogeography at the junction between Alpine Tethys and Pyrenean Rift

Nicola Mondillo [a,b,*], Cyril Chelle-Michou [c], Francesco Putzolu [b], Giuseppina Balassone [a,d], Angela Mormone [d], Licia Santoro [e], Salvatore Cretella [a], Gennaro Scognamiglio [a], Marcella Tarallo [a], Stefano Tavani [a]

[a] Dipartimento di Scienze della Terra, dell'Ambiente e delle Risorse, Università degli Studi di Napoli Federico II, 80126 Napoli, Italy
[b] Department of Earth Sciences, Natural History Museum, SW7 5BD London, UK
[c] Institute of Geochemistry and Petrology, Department of Earth Sciences, ETH Zurich, 8092 Zurich, Switzerland
[d] INGV Osservatorio Vesuviano, 80125 Napoli, Italy
[e] Dipartimento di Scienze della Terra, Università di Torino, 10124 Torino, Italy

ARTICLE INFO

Article history:
Received 19 December 2023
Revised 7 September 2024
Accepted 29 September 2024
Available online 1 October 2024
Handling Editor: L. Tang

Keywords:
Bauxite
France
Cretaceous paleogeography
U-Pb zircon dating
Pyrenean Rift

ABSTRACT

Karst bauxites mark episodic exhumation of carbonate platforms, thus providing key information for basin analysis and paleoclimate processes at the regional to continental scale. Most karst bauxite deposits of SE France lie between Jurassic platform carbonates in the footwall and Upper Cretaceous marine to continental sediments in the hanging wall. These deposits delineate a stratigraphic gap coeval with the Durance extensional tectonics, which led to the separation of the Vocontian and South Provence Basins, and shaped the junction between the Alpine Tethys and the Pyrenean Rift.

Our new mineralogical and geochemical data show that SE France karst bauxites were affected by in-situ weathering and alteration in conjunction to sedimentary reworking. Statistical analysis of geochemical data indicates that bauxite deposits have a similar chemical footprint, likely pointing to a common and long-lasting bauxitization process. New U-Pb zircon data from the Provence deposits confirm that the source material for the SE France bauxites is to be primarily found in the Hercynian basement. The data suggest the presence of an additional exotic zircon source deriving either from Avalonia and/or Baltica. The comparison of the new U-Pb zircon data with those on coeval bauxites evidences a marked difference between the SE France and the Sardinian deposits. This difference indicates diversification in the detritus provenance of the two areas since the Lower Cretaceous, setting the bauxites of SE France and Sardinia in lateral continuity with the bauxites occurring on the two opposite margins of the Pyrenean Rift, and supporting the development of these deposits on the shoulders of the rift-related basin formed at the eastern termination of the Pyrenean Rift.

1. Introduction

The paleogeography of the junction between the Alpine Tethys and the Pyrenean Rift, including the Sardinia-Corsica block's positioning and its kinematic relationship with neighboring areas such as, for example, the SE France Basin, are subjects of discussion in the context of tectonic reconstructions of the Western Mediterranean in the mid-Cretaceous period. The discussion largely relates to the long-debated timing and mode of connection between the Bay of Biscay-Pyrenean Rift, the Iberian Rift, the Alpine Tethys, and the Valais Ocean during the mid-Cretaceous (Fig. 1). Various scenarios exist (Fig. 1), which place the Sardinia-Corsica block either within Iberia (e.g., Stampfli and Borel, 2002; Schettino and Turco, 2011), Eurasia (e.g., van Hinsbergen et al., 2020), or within the almost independent Ebro crustal block placed in between (e.g., Tavani et al., 2018; Angrand and Mouthereau, 2021). The coexistence of different and irreconcilable hypotheses arises from the complexity of the late Cretaceous to Cenozoic tectonic history of the area (e.g., Handy et al., 2010; van Hinsbergen et al., 2020), which includes Alpine (e.g., Schmid et al., 2004) and Pyrenean oro-

* Corresponding author.
E-mail address: nicola.mondillo@unina.it (N. Mondillo).

https://doi.org/10.1016/j.gr.2024.09.012
1342-937X/

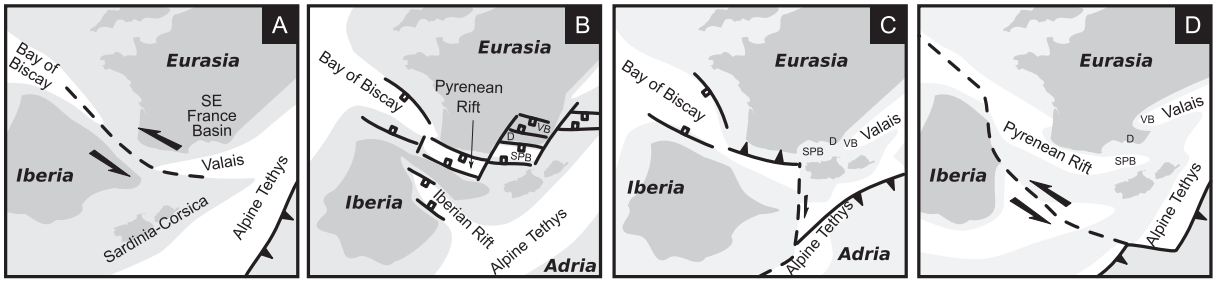

Fig. 1. Reconstructions of the Iberia-Eurasia-Adria junction area, with position of the Sardinia-Corsica block and SE France Basin at the mid-Cretaceous time. a) After Stampfli and Borel (2002). B) After Tavani et al. (2018). C) After van Hinsbergen et al. (2020). D) After Angrand and Mouthereau (2021). Abbreviations: D = Durance Isthmus, SPB = South Provence Basin, VB = Vocontian Basin.

genesis (e.g., Bestani et al., 2016; Balansa et al., 2022), and late Oligocene to Miocene opening of the Liguro-Provençal Basin and drifting of the Sardinia-Corsica block away from the SE France Basin (Gattacceca et al., 2007; Bache et al., 2010; Jolivet et al., 2015). Such a severe tectonic overprint poses challenges to correlations between the tectono-sedimentary record of the various areas (e.g., Costamagna, 2023), and to restoration of the position of the main basins and structures. The extensive sedimentary gap that occurred during the mid-Cretaceous period in response to local uplifts makes it even more difficult to compare the sedimentary succession of the different areas. In this context, constraints for basin analysis and plate tectonic reconstruction can be obtained by studying the provenance of the mid-Cretaceous bauxite deposits that developed during this gap and their time–space distribution with respect to the main basins.

Bauxites are residual deposits containing economic concentrations of aluminum hydroxides (gibbsite, boehmite or diaspore), deriving from deep weathering of aluminosilicate parent rocks, under humid, tropical to subtropical climates (Bárdossy, 1982; Bárdossy and Aleva, 1990; Herrington et al., 2016). Although recent bauxites can be found associated to lateritic soil profiles overlying the weathered parent rocks, in old sedimentary records bauxites can occur interbedded to platform carbonate rocks. These deposits, which are known as "karst bauxites", lack an unweathered protolith at their basis and mark local disruption of marine sedimentation and the establishment of transitional to continental environments. For this reason, karst bauxites generally mark stratigraphic gaps within the carbonate succession (e.g., Cretaceous bauxites in the Mediterranean realm; Bárdossy, 1982; Bárdossy and Aleva, 1990; Herrington et al., 2016). Being necessarily associated with episodic exhumation of the carbonate platforms, karst bauxites are considered excellent tools for reconstructing geodynamic and paleoclimate processes at the regional to continental scale (e.g., Bárdossy and Aleva, 1990) and have been widely used for conducting provenance investigations aimed at determining the nature of the parent rocks and their paleogeographic position (e.g., Boni et al., 2013; Zhang et al., 2017; Wang et al., 2018; Shamanian and Hattori, 2021; Marchand et al., 2021; Yang et al., 2022; Yu et al., 2023; Wang et al., 2023).

Here, we report on the existing data on the SE France bauxite deposits occurring at the junction between the Alpine Tethys and the Pyrenean Rift and integrate them with new geochemical data on Provence and Languedoc bauxites (Fig. 2), as well as new U-Pb data of detrital zircons of the Provence deposits, to support provenance investigations (e.g., Li et al., 2017; Liao et al., 2017; Zhang et al., 2019). The bauxites of SE France are boehmite-gibbsite-bearing karst-type deposits associated with a regional stratigraphic gap of Early to mid-Cretaceous age (Nicolas, 1968; Guendon and Parron, 1985; Combes, 1990). This gap is related to an episode of extensional tectonics, known as the "Durance phase" (e.g., Combes, 1990), which formed a tectonic high, i.e., the "Durance Isthmus", separating the Vocontian and South Provence Basins (Tavani et al., 2018, and references therein) (Figs. 1, 2). The French bauxites formed from the alteration of siliciclastic sediments deposited on tectonically uplifted carbonate platforms and were lately affected by reworking and re-sedimentation within the karst network (Nicolas, 1968; Guendon and Parron, 1985; Combes, 1990; Chanvry et al., 2020; Marchand et al., 2021). The siliciclastic sediments are considered to have originated from the erosion of the exposed Hercynian basement (e.g., Massif Central, Maures Massif), outcropping in areas located nearby the carbonate platforms (Nicolas, 1968; Guendon and Parron, 1985; Combes, 1990; Marchand et al., 2021). Although there is a general agreement on these statements, a debate exists on some aspects regarding the genesis of the bauxite deposits and also on the origin of the source material. Specifically, for certain authors (e.g., Guendon and Parron, 1985) the SE France bauxites are *autochthonous* (i.e., they derive from in-situ alteration of sediments that covered the carbonate platforms), for some authors (e.g., Nicolas, 1968; Chanvry et al., 2020) they are *allochthonous* (i.e., bauxites formed in the French inland from the direct alteration of the basement, and were lately eroded and mechanically accumulated on the carbonate platforms), for other authors (e.g., Combes, 1990) bauxite deposits derive from a mixing of these two end-member models, and must be considered *parallochthonous* or *parautochthonous* deposits. Regarding the possible source rocks for the bauxites, the competing hypotheses are: 1) the Hercynian basement – with its various massifs, and 2) Cretaceous marls overlaying the carbonate platforms and the basement itself (Marchand et al., 2021, and references therein). These models directly impact the paleotectonic and paleogeographic reconstruction of the southern France margin during the mid-Cretaceous. Indeed, the provenance of the parent source material at the time of deposition depends on the presence of possible exhumed source rocks and on the pattern of the fluvial to marine systems. For example, the recent paper of Marchand et al. (2021) proposed that during the Barremian-Aptian interval, moderate uplift of the southern France margin led to weathering of a thick portion of the carbonate platform succession and the marly sedimentary cover. During the Albian, the formed bauxites were mechanically deposited in karst cavities and enhanced uplift and denudation also exposed the basement to erosion. Yu et al. (2023), which report U-Pb data of detrital zircons of Sardinia bauxites, stated that Sardinia was located on the prolongation of the Durance Isthmus, and proposed that the main source rocks of bauxites were located in the Massif Meridional as the structural relics in the allochthonous slices of basement in the Maure Massive and in basement outcrops buried in the Liguro-Provencal Basin. These models are based on various paleogeographic reconstructions of the southern European margin during mid-Cretaceous, which differ on: 1) the possible extension of the Vocontian Basin

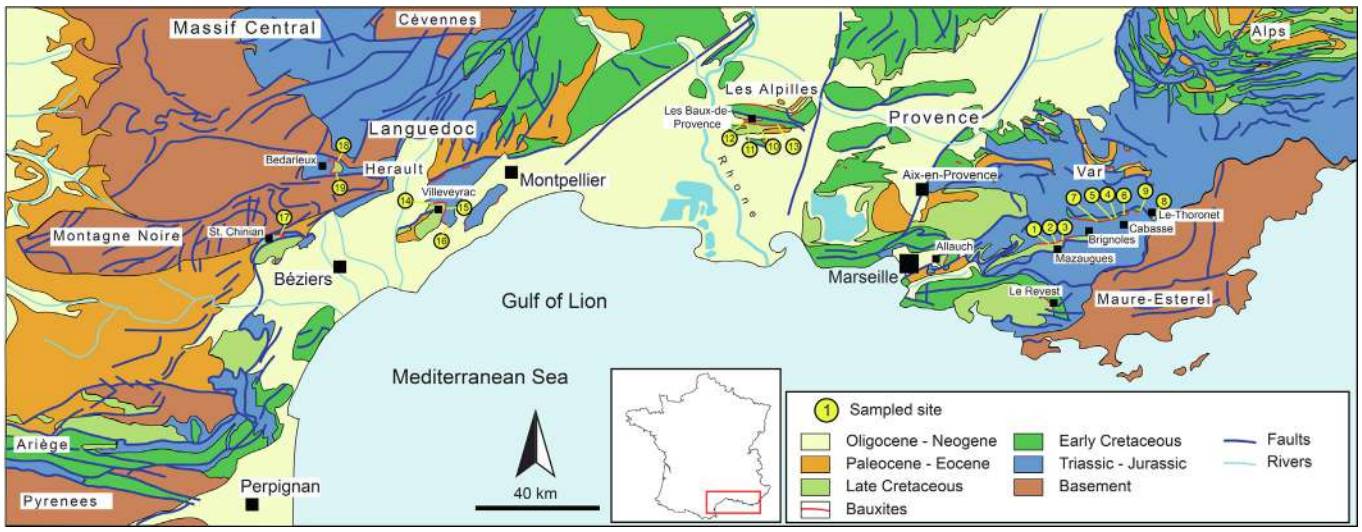

Fig. 2. Geological map of southern France (Modified from BRGM, 2005). Sampled sites: 1) Mazaugues – Calas-la Caire; 2) Mazaugues – Les Feuilles – Mazaugues Amont; 3) Mazaugues – le Baume de Saint Michel; 4) Brignoles – Brauch; 5) Brignoles – Brauch Cabasse; 6) Brignoles – Combecave; 7) Brignoles – Lac Saint-Christophe; 8) Le Thoronet – Le Rigoulier; 9) Le Thoronet – Peygros; 10) Les Baux de Provence – Anticlinal de Manville; 11) Les Baux de Provence – Mas de l'Oulivie; 12) Les Baux de Provence – Les Canonnettes; 13) Les Baux de Provence – Le Destet; 14) Villeveyrac L'Olivet; 15) Villeveyrac Mas de Veirier; 16) Loupian; 17) Saint Chinian; 18) Bedarieux Carlencas-et-Levas; 19) Bedarieux La Braunhe.

in the Valais ocean; 2) the position of the Sardinia-Corsica block relative to the Durance Isthmus; and 3) the possible linkage between the Sardinia-Corsica block and Iberia (Fig. 1). Our new data on Provence and Languedoc bauxites aim to: 1) determine genetic processes at a regional scale; 2) locate the possible bauxite source rocks; and 3) improve the knowledge on the paleogeography of the junction between the Alpine Tethys and the Pyrenean Rift during the Cretaceous after comparison with the existing studies.

2. Geological setting and summary of previous studies on SE France bauxite deposits

2.1. Summary of the regional geology

The Provence and Languedoc bauxite districts are located in southern France, between the easternmost portion of the Pyrenees and the foreland of the Western Alps (Fig. 2). In both areas, the present structural framework is a result of the Late Cretaceous to Eocene Pyrenean compression (e.g., Lacombe and Jolivet, 2005; Espurt et al., 2012) and, in Provence only, of the Cenozoic Alpine compression (e.g., Bergerat, 1987; Champion et al., 2000). The Oligocene extension (West European rifting, and Liguro-Provencal rifting) separated the above-mentioned tectonic events (Hippolyte et al., 1993; Séranne, 1999; Gattacceca et al., 2007). Regional-scale structures were reactivated multiple times during Jurassic, mid-Cretaceous tectonics, Pyrenean shortening and Oligocene rifting (e.g., Hemelsdaël et al., 2021).

The bauxite districts are bordered by metamorphic and igneous rocks of the Hercynian basement, belonging to the Maures (Maure-Esterel) and Tanneron Massifs in Provence, and to the French Massif Central (Cévennes and Montagne Noire highs) in Languedoc (Faure et al., 2009) (Fig. 2). Late Carboniferous to Permian volcanoclastic series, deposited during the rifting of Gondwana, unconformably overly basement rocks (e.g., Bruguier et al., 1998, 2003; Delfaud et al., 1989), and are in turn covered by Mesozoic to Quaternary sedimentary rocks (e.g., Beaudrimont and Dubois, 1977; Cotillon, 1984; Bonijoly et al., 1996; Bourquin et al., 2011). Footwall units of bauxites include Triassic to Early Cretaceous sedimentary sequences, while Late Cretaceous to Eocene sediments

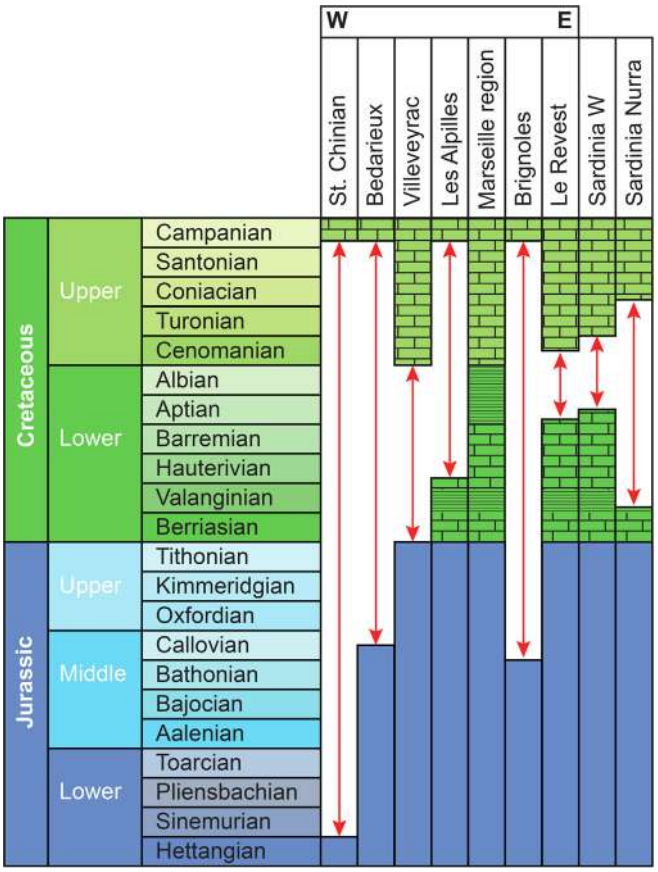

Fig. 3. Correlation between sedimentary series and stratigraphic gaps in the study areas (BRGM; Combes, 1990; Guyonnet-Benaize et al., 2010). For the age of the sedimentary cover of the Villeveyrac bauxite refer to Marchand et al. (2021).

represent hanging wall lithologies (Combes, 1990) (Fig. 3). In Provence, the Triassic to Early Cretaceous successions have a total thickness of ca. 2 km; they include Triassic red sandstones, shales, and evaporites, Liassic to Middle Jurassic marine limestones and

black shales, Late Jurassic marine limestones, Berriasian marine limestones, Valanginian yellow marine limestones and shales, and Barremian to Aptian marine limestones and shales (Espurt et al., 2012). In Languedoc, the Jurassic succession is dominated by marine carbonates and early Neocomian marls; the Early Cretaceous (Valanginian to Hauterivian) is dominated by marls and marly limestones (Beaudrimont and Dubois, 1977; Mascle et al., 1996; Arnaud et al., 1984; Cotillon, 1984). As shown by Barbarand et al. (2001), and recently confirmed by Barbarand et al. (2020), the Jurassic to Early Cretaceous sedimentary rocks extended over the southern Massif Central, including the Causses domain and the Hercynian basement at the borders of the Aquitaine and South-East basins. In these areas, the sedimentary cover had a significant thickness (variable from 1 to 2 km depending on the area), but was characterized by low bathymetry facies due to balance between sedimentation and subsidence (Barbarand et al., 2020).

During mid-Cretaceous, a large geodynamic reorganization in the South-East Basin, i.e., the Durance phase, led to the formation of an elongated horst, i.e., the Durance Isthmus, which separated the Vocontian Basin from the South Provence Basin, while connecting the French Massif Central to the west, and the Maures (Maure-Esterel) Massif to the east (Masse and Philip, 1976; Guyonnet-Benaize et al., 2010, 2015; Espurt et al., 2012; Bestani et al., 2016). This tectonic phase occurred in response to Early to mid-Cretaceous divergent movements in the easternmost portion of the Iberia-Eurasia plate boundary (Tavani et al., 2018). The Durance uplift stage produced widespread exhumation and erosion of sedimentary rocks deposited in the Mesozoic basins on the southern border of the French Massif Central and denudation of the basement (Curnelle and Dubois, 1986; Barbarand et al., 2001; Peyaud et al., 2005; Olivetti et al., 2020; Barbarand et al., 2020). The transition between the Jurassic and the Cretaceous in the Aquitaine Basin is marked by a regional unconformity. An extensive karstification correlated to this unconformity in the underlying Jurassic sedimentary rocks is observed in the eastern border of the Aquitaine Basin (Simon-Coinçon et al., 1997). The level of erosion is variable in the different portions of the basin: Upper Jurassic in the Causses domain, mainly Lower Jurassic in the Rodez Strait, Middle Jurassic in the Cévennes High (Barbarand et al., 2020). The entire sedimentary section was removed from the Cévennes and Rouergue basements (Barbarand et al., 2020). The Languedoc and Provence bauxite deposits occur in correspondence of this unconformity (Combes, 1990). The erosional hiatus locally extends here down to the Jurassic (Sinemurian), confirming the km-scale uplift and denudation (Masse and Philip, 1976; Combes, 1990) (Fig. 3). The youngest strata underlying the bauxite deposits are Barremian in age (Philip et al., 1978; Lajoinie and Laville, 1979).

The bauxite deposits were then covered by continental to shallow marine Late Cretaceous sediments (mostly sandstones, marls, and carbonates, also with few conglomerates; Combes, 1990). Most commonly, the sedimentary cover has a Santonian-Campanian age (Combes, 1990), although it spans from the Aptian in the Pyrenees (Combes, 1990), to the Turonian in Provence (Lajoinie and Laville, 1979), and even to Eocene in the Bédarieux zone (Combes, 1969). Recent absolute dating provides a Late Albian age for the cover of the Villeveyrac bauxites (Marchand et al., 2021).

2.2. Previous studies on southeastern France bauxite deposits

The discovery of France bauxites in the Alpilles mountains is credited to Bertier (1821). Further geological investigations were conducted in the second half of the 19th century (e.g., Stevard, 1863; D'Aoust, 1865; Daubrée, 1869; Coquand, 1871), with Dieulafait (1881) who firstly proposed a weathering-related origin of the French bauxites. Modern, still pioneering, scientific investigations were published between 1960 and 1990: e.g., Valeton and Klint (1962); Rousset (1968, 1969); Nicolas (1968); Combes (1969, 1972, 1973, 1984, 1990); Lajoinie and Laville (1979); Laville (1981); Guendon and Parron (1985). Valeton and Klint (1962) firstly recognized two types of bauxite deposits: 1) deposits filling large and deep karst cavities (e.g., Bédarieux), and 2) thin lenticular bodies extending for wider areas (e.g., Mazaugues). Looking in detail at the Mazaugues deposit, it was also recognized that the bauxite body was characterized by a vertical zonation associated with distinct degrees of alteration, resembling the structure of a lateritic profile: the base was enriched in kaolinite, the central horizon was richer in Al- and Fe-(oxy)-hydroxides in the form of pisolites and oolites, whereas the topmost layer consisted of yellowish clayey material. From these characteristics, the authors suggested that bauxite was formed through in-situ weathering, likely at the same time or slightly after the karstification of the bedrock limestone. The lacustrine sedimentary cover contained lignite lenses.

Nicolas (1968) is one of the first authors to propose a sedimentary nature of the SE France bauxites. This author, investigating the structure and textures of the deposits located in the Brignoles area (Var), evidenced the diffuse occurrence of conglomeratic and pisolitic facies, and the existence of sedimentary breccias, detrital fossils, broken grains, and sedimentary structures within the bauxite layers (e.g., gradation). All these features suggested that bauxites resulted from the erosion, transport, and deposition (in an aqueous medium) of former lateritic bauxites above karstified limestones.

Guendon and Parron (1985) conducted detailed multiscale investigations of the Canonettes and Fléchons deposits (Alpilles). They showed that in the investigated bauxites: 1) kaolinite was often underlying the pisolitic bauxite horizon, as in the typical lateritic bauxite profiles; 2) the karstified limestones in the footwall had funnel-shaped depressions, indicating dissolution under cover; 3) the bauxite proximal to the centers of the karstic depressions was richer in gibbsite and pisolites and poor in silica: it was therefore more evolved than bauxite occurring on the sides of the paleo-karst cavities. This suggested that groundwaters were flowing through the bauxitic horizons toward the center of the cavities, producing in-situ alteration during ongoing karstification. Following these earlier studies, the extensive work carried out mainly by P.J. Combes (e.g., Combes, 1969, 1972, 1973 – summarized later), but also by other authors, Lajoinie and Laville (1979 – see internal references) published the first inventory of bauxite deposits of the SE France (followed later by Lajoinie and Laville, 1980 and Laville, 1981, who also published drillcore data). The compilation reports tonnages and grades of the bauxite mines active in France in the 1980s, the descriptions of the facies and mineralogical assemblages, as well as the regional and local geological maps and sections. Lajoinie and Laville (1979) showed that a common lithological feature among several SE France bauxites is represented by the occurrence of three distinct pseudo-layered facies within most of the ore bodies: a) upper siliceous facies, mostly composed by kaolinite, b) median bauxitic facies, mostly consisting of boehmite, and less gibbsite, characterized by conglomeratic, pisolitic or/and oolitic structures, and c) lower siliceous facies, made of kaolinite, with subordinate Al-hydroxides, directly overlying the carbonate bedrock. These facies show a variable thickness among the different bauxite deposits, and are chemically marked by different silica contents (in the siliceous facies the contents are higher than in the median bauxite). The carbonate bedrock was commonly affected by karstification. Commonly, the rocks conformably overlying the bauxite horizons were represented by fine clastic lacustrine sediments, which could also have contaminated the topmost bauxite layers through *per descensum* alteration processes. On the basis of these observations, Lajoinie and Laville (1979) suggested that the materials from which the bauxites orig-

inated could be represented by lateritic soils rich in kaolinite formed either above (in-situ) or close to the carbonate platforms. Bauxite deposits were derived from the pervasive drainage of these kaolinitic soils, or from the mechanical transport and remobilization of the *autochthonous* bauxitic material in nearby karst depressions.

Combes (1990) in a synthesis of his own studies (e.g., Combes, 1969, 1972, 1973) and of those of other authors (Valeton and Klint, 1962; Rousset, 1968, 1969; Nicolas, 1968; Lajoinie and Laville, 1979; Laville, 1981; Guendon and Parron, 1985), depicted a general setting for the genesis of the bauxites in SE France. This author emphasized how the type and origin of these bauxite deposits depend on the base level of the erosion, and on the degree of tectonic activity at the time of deposit formation. While the Languedoc and Provence bauxites were interpreted to derive from the ferralitization of the post-Hercynian siliciclastic sedimentary cover of the basement, their genesis was considered to have been influenced by the uplift rate and by the acting drainage. Combining high/low uplift rates, high/low drainages, erosion and deposition, different types of bauxite deposits could be formed: *autochthonous*, *parautochthonous* or *allochthonous*. Making a comparison at a regional scale, Combes (1990) considers only Sardinia bauxites as *autochthonous* deposits, as they directly formed at the expense of Valanginian to Berriasian green marls, conformably covering the Jurassic carbonate bedrock. Following the author's scheme, Languedoc and Provence bauxites were considered *parautochthonous* or *allochthonous*. This means that they derived from erosion, transport, sedimentation (allochthony) and eventually from secondary in-situ alteration (parautocthony) of Sardinian-type deposits (in this case deriving from the alteration of Early Cretaceous marls), or of residual profiles formed in-situ above the basement, e.g., Montagne Noire in the Languedoc region, or the Maure-Esterel Massif in the Provence region, at the expense of the Hercynian rocks or of their sedimentary cover. Combes (1990) also proposed the term "parallocthony" for designating bauxites developed from in-situ weathering of Early Cretaceous marls, at the same time as the karstification of the underlying carbonate footwall. *Parautochthonous* or *allochthonous* deposits were developed in areas affected by high uplift rates, whereas *autochthonous* bauxites prevailed in areas of low uplift rates. The strong ferralitization and silica leaching in the continental areas was associated with the precipitation of glauconite in surrounding marine environments (Combes, 1990).

Thiry et al. (2006) and Ricordel-Prognon et al. (2010) conducted studies at the sub-continental scale for correlating SE France bauxites with other Cretaceous lateritic deposits located in the European inland. In particular, they initially inferred (Thiry et al., 2006), then confirmed by paleomagnetic dating (e.g., Ricordel-Prognon et al., 2010), that iron-rich lateritic bauxite profiles and ferruginous kaolinitic paleosoils overlying the basement rocks of the French Massif Central were of Late Jurassic to Early Cretaceous in age (140–160 Ma with a confidence limit of 10 Ma), which is much older than the previously assumed Eocene-Oligocene age. From a paleoclimatic perspective, Early Cretaceous Fe-rich lateritic paleosoils could be correlated with the karst bauxite deposits of southern France, suggesting a long-lasting continental evolution and a climatic and landscape stability. The presence of various types of Cretaceous lateritic paleosoils on the Massif Central was considered to reflect a lack of sedimentary cover above the central part of the French Massif Central at the Jurassic-Cretaceous boundary. Moreover, the low compaction of the profiles was ascribed to the absence of burial beneath a significant sedimentary cover, pointing to a stability of some areas of the French Massif Central throughout the Mesozoic (Ricordel-Prognon et al., 2010). Conversely the neighboring basins (e.g., Aquitaine and Paris), as well as blocks of the basement itself, were subsided about 2000 m (Barbarand et al., 2020).

More recently, Marchand et al. (2021) presented the results of detrital zircon U-Pb dating on Languedoc bauxites to investigate the nature of their parent rock. The authors determined ages ranging from 113 Ma to 3.5 Ga, and five age clusters centered on 350 Ma, 600 Ma, from 1,000 to 1,200 Ma, between 1,600 and 1,900 Ma, and 2,700 Ma. The presence of detrital zircon grains with young ages (ca. 115 Ma) in the Bédarieux bauxite confirmed that bauxites were deposited between 115.5 Ma (i.e., Aptian) and late Albian, after reworking and trapping in the Languedoc basins for a period of ca. 10 Myr. Older zircon grains were considered to be associated with parent rocks occurring in the Montagne Noire and with other protoliths of the European continental crust. Zircons of late Mesoproterozoic, Paleoproterozoic and Archean ages were considered of problematic interpretation, this because, according to Marchand et al. (2021) similar ages have never been found in previous U-Pb studies from the Hercynian basement. This age spectrum was explained supposing the existence of two distinct sources: a localized source in the Hercynian basement of the Montagne Noire, and a generalized sedimentary source, characterized by four significant age-clusters: i.e., Late Neoproterozoic, Late Mesoproterozoic, Paleoproterozoic and Neoarchean. The latest was considered by the authors as a regional, homogeneous, sedimentary cover, extending across the present outcrops of Hercynian basement in the French hinterland, and the Mesozoic Tethyan carbonate platform, and represented by the Valanginian marls and marly limestones. This hypothesis was consistent with the widespread sedimentary cover, earlier proposed by Barbarand et al. (2001). According to Marchand et al. (2021), the alteration of the Valanginian sequence supplied a significant fraction of the material for bauxite generation. In particular, between Late Aptian to Early Albian marls and clays occurring on the Hercynian basement were weathered and transformed into lateritic bauxites, while carbonate platforms were mostly subjected to uplift and karstification. In the Early Albian, due to tectonic instability, lateritic bauxite material was eroded from the basement cover, and accumulated above the karstified carbonate platforms forming *allochthonous* karst bauxite deposits (Marchand et al., 2021).

Chanvry et al. (2020) presented a detailed sedimentary facies model obtained on a representative drillcore from the Villeveyrac bauxite basin. The authors distinguished depositional facies and sedimentary features (i.e., broken blocks of iron crusts and pisolites in a mud matrix) indicating mechanical transport, compatible with mass-flow sedimentation processes. Mineralogical analyses revealed a vertical zonation of the bauxite layer, that was characterized by the decrease of Al- and Fe-oxy-hydroxides from the bottom to the top, correlated with the increase of kaolinite in the same direction. Bauxite cover resulted much richer in silica, associated with the presence of smectite clays and quartz, and had textural features indicating in-situ pedogenesis. Considering all these features, the authors proposed that the bauxite layer formed through progressive stripping of lateritic profiles in the hinterland and reverse stacking, as a detrital sequence, into the karstic trap, thus confirming the *allochthonous* depositional model. This model was also used to explain the widespread relationships (positive and negative correlations) between major oxides observed in other drillcores from the same basin (Marchand, 2019). On the contrary, the paleosoil overlying the bauxite interval accounted for both the change in depositional and climate conditions (Chanvry et al., 2020). Deferrification features, occurring at the top of the Villeveyrac bauxite body, were mostly correlated with post-depositional processes started since the deposition of the silica-rich cover above the bauxite. On the contrary, fracture-controlled deferrification likely formed after bauxite lithification, after circu-

lation of fluids during the Oligocene extensional tectonics (Marchand, 2019). In these studies, it was recognized that karstification of the Jurassic carbonates was both isotropic and fracture-controlled, following NE-SW and NW-SE striking joints (Marchand, 2019). At the same time, the formation of the large bauxite deposits of the Villeveyrac area was considered to be controlled by the development of local grabens bordered by NW-SE-striking *syn*-sedimentary fault systems (Marchand, 2019; Marchand et al., 2021).

Looking at the tectonic setting at the time of bauxite formation, a distinct situation was documented by Guyonnet-Benaize et al. (2010) in the Allauch Massif-Marseille region, in Provence. By using restored 3D models, it was shown that several bauxite deposits were aligned along a NW-SE trend, which corresponded to the bedding strike of Lower Cretaceous sedimentary rocks during the Durance uplift. Specifically, in this area the Durance tectonics likely produced normal faulting and tilting of Lower Cretaceous beds. Bauxites were not preserved directly in sags along normal faults, but in steps and karsts striking NW-SE, which were dug by aerial erosion crosscutting to the SW-dipping tilted strata.

3. Main features of the studied bauxite horizons

In Provence, bauxite was sampled in several areas in the Var department and the Les Alpilles. In the Var department, deposits are located in the Mazaugues area and in several localities northeast of Brignoles including Le Thoronet, Saint Christophe, Cabasse-Brauch and Combecave areas (Fig. 2). North of the Mazaugues village, two distinct sites were investigated: the Calas-la Caire (NW Mazaugues) and the Les Feuilles (NE Mazaugues) old mine pits. The same bauxite horizon crops out in the latter localities, where it overlies Late Jurassic carbonate rocks and is covered by Turonian limestones (Lajoinie and Laville, 1979). At both sites, the bauxite body was sampled along vertical profiles perpendicular to the main horizon. At the NW Mazaugues (Calas-la Caire), the upper section of the bauxite horizon was well exposed, whereas its lower contact was not observed. The sampled bauxite horizon has a thickness of about 3 m and is composed of a clayey and massive upper pseudo-layer (1 m), overlying a conglomeratic-pisolitic lower horizon (about 2 m) (Fig. 4A). Bleaching structures were common in both outcrops. Bauxite is overlain by 50 cm of stratified limestones, containing bauxite clasts and fossil gastropods. At NE Mazaugues (Les Feuilles), in the old open pit, remnants of the bauxite horizon crop out, where both the upper and lower contacts are still visible. The sampled bauxite is marked at the top and at the bottom by thin pseudo-layers of the more clayey facies. The median bauxite body, as at NW Mazaugues, has a conglomeratic to pisolitic structure: centimetric nodules and pisolites are scattered in a reddish to whitish matrix (Fig. 4B). The nodules have a red color, pisolites are reddish to black, and both show complex concretionary structures. Also in this outcrop, the bauxite matrix shows bleaching streaks. The underlying carbonate rock is altered and has an irregular morphology, characterized by rounded surfaces, with bauxite infills into cracks.

Bauxites occurring northeast of Brignoles (Fig. 2) overlay the Jurassic carbonate rocks, and are in turn covered by Late Cretaceous limestones, as in Mazaugues (Fig. 3). In the le Thoronet, Combecave and Cabasse-Brauch areas, bauxite marks the Bathonian-Campanian stratigraphic gap (Lajoinie and Laville, 1979), whereas in the Saint Christophe area the carbonate cover is Turonian-Coniacian in age (Lajoinie and Laville, 1979). In the le Thoronet area, bauxite was sampled in two old mine pits (Peygros and Rigoulier), from remnants of the median bauxite body. In the Peygros pit, bauxite shows bleaching structures, whereas in the Rigoulier pit, it was possible to observe sedimentary structures within the bauxite median body. Specifically, the reddish bauxitic material is finely intercalated with clastic carbonate layers with a mm- to cm-scale grain size and sub-rounded shapes. Between the Vins and Cabasse villages, several bauxite outcrops can be observed along the D24 road. Even though the bauxite body was not fully exposed, several erratic samples were collected at various sites in the Saint Christophe, Cabasse-Brauch (from the lower section of the horizon), and Combecave (from the lateral section of the horizon) areas. At Cabasse-Brauch, the exposed bauxite horizon has a thickness of about 10 m, a reddish color, and is off-set from the basal carbonate rock by a 2 m thick macro-breccia made of limestone blocks dispersed in a bauxite matrix. Bauxite is more clayey at the base of the horizon and in the higher part, even though the upper contact with limestones was not observed. In this outcrop, bleaching streaks have a limited extent (Fig. 4C). The Combecave outcrop includes both the basal and the upper contacts with carbonate rocks. The horizon has a thickness of about 5–6 m and consists of a median bauxite body, underlain by a clayey bauxite, and overlaid by a clay layer (about 2 m). Bauxite fills fractures and cracks of the underlying Jurassic carbonate rock, which have a regular pattern (Fig. 4D), likely controlled by synchronous Cretaceous extensional tectonics at a local scale (Tavani et al., 2018). In the Saint Christophe area, it was not possible to observe the bauxite horizon at a full extent: only erratic samples were collected from the median bauxite body.

In Les Alpilles area (Fig. 2), nearby Les Baux de Provence, the investigated bauxites were sampled from two outcrops of the same bauxite horizon in the Les Canonnettes old mine site, and along the D78F and D5 roads. The sampling sites are called Mas de l'Ouliviè and Anticlinal de Manville. Here the bauxite horizon overlies the Hauterivian to Barremian limestone, and is covered by Coniacian limestone (Combes, 1990) (Fig. 3). At Les Canonnettes, several samples were collected from the horizon outcropping on the eastern side of the pit, for about 15 m in a direction perpendicular to bauxite layering, from the overlying limestone to the bottom of the mineralized horizon. The section is not continuous because the road that gives access to the pit crosscuts the horizon: samples were therefore collected from the central body below the road (Fig. 4E) and from the upper section, above the road (Fig. 4F). The contact of the bauxite with the underlying limestone was not exposed and could not be sampled. Bauxite is clayey at the top (Fig. 4F), whilst it is more granular and pisolitic at the center. The Anticlinal de Manville outcrop is a good example where the basal contact of the local bauxite horizon with the carbonate rock can be traced. Here, lenticular to irregular clastic to pisolitic bauxite bodies are common. These bodies cut the Lower Cretaceous limestone strata for about 10 m, and locally fill cracks or occur as the matrix component of breccia with carbonate clasts. The Mas de l'Ouliviè bauxite was similar to the orebody occurring at the Anticlinal de Manville. Another outcrop of the lateral extension of the Les Canonnettes horizon was sampled in the Le Destet area, where the bauxite is a much thinner (about 1 m) horizon, reddish, clayey and carbonaceous.

In the Languedoc, the sampled bauxites are located in the Herault area, nearby Bédarieux, Saint Chinian-Pierrerue, Villeveyrac, and Loupian (Fig. 2). Near Villeveyrac, the bauxite outcrops occur on the north and east borders of the Villeveyrac basin, in the localities of L'Olivet and of Mas de Veirier respectively, along the D2 road (Fig. 2). At both sites, the bauxite horizon crops out in a syncline, which folds the Mesozoic to Paleogene sedimentary succession (Lajoinie and Laville, 1979). This bauxite occurs at the hanging wall of Tithonian carbonate rocks, and is covered by Late Albian limestones (Combes, 1969; Marchand et al., 2021) (Fig. 3). The L'Olivet outcrop includes several bauxite pockets infilled in dm- to m-sized karst cavities within the carbonate footwall. These cavities locally have an elongated shape and subvertical orienta-

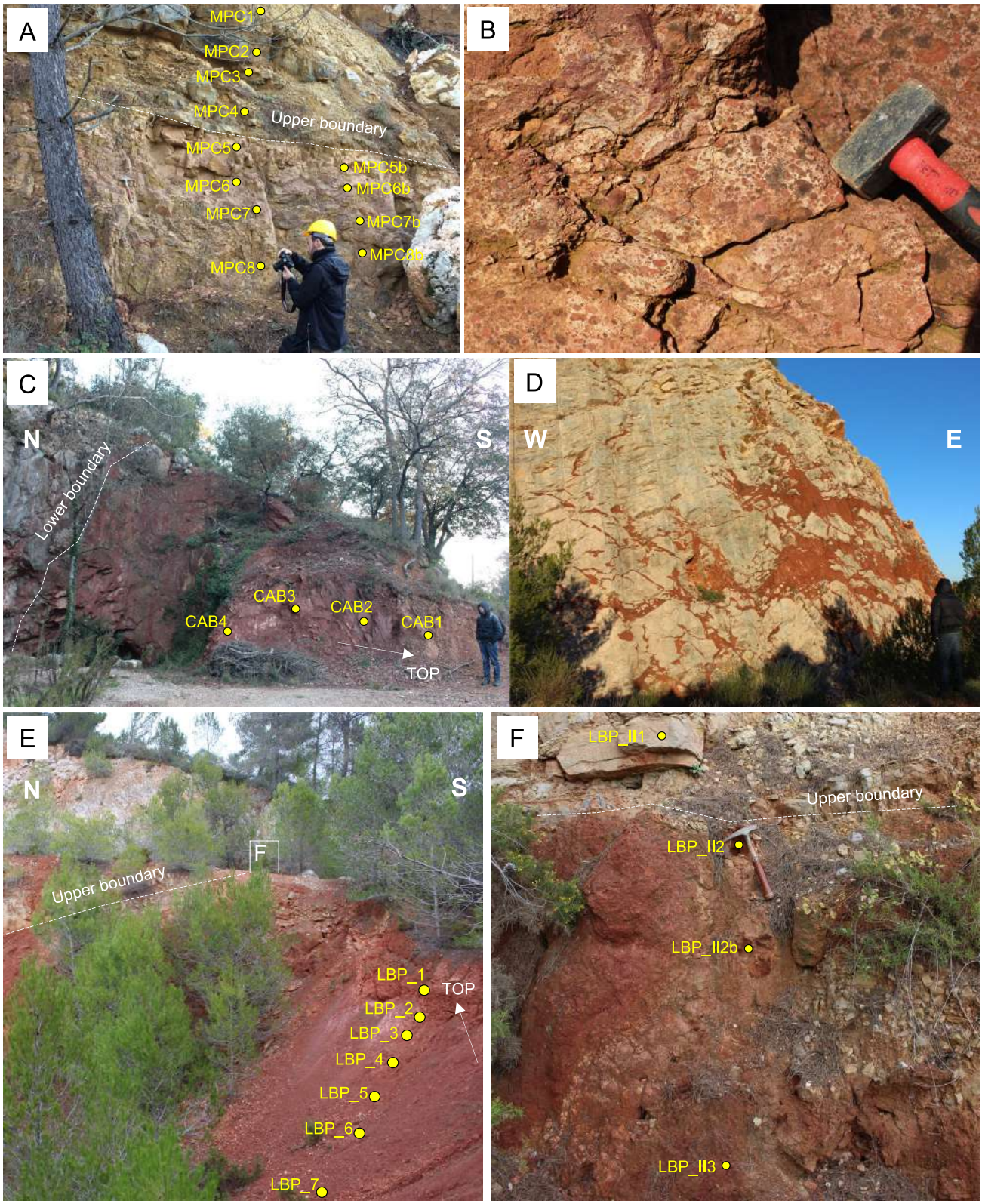

Fig. 4. Examples of bauxite outcrops in Provence, with the positions of the collected samples. Var department: A) NW Mazaugues – Calas-la Caire pit: upper section of the bauxite horizon. B) NE Mazaugues – Les Feuilles pit: bauxite with a conglomeratic to pisolitic structure (see sample MAM 1a). C) Brignoles – Cabasse-Brauch (small pit along the D24 road): subvertical bauxite horizon with an E-W orientation. The white arrow indicates the polarity of the layer: the basal limestone is on the left of the image, whereas the cover is not exposed. D) Combecave pit (Lac de l'ancienne Mine): the outcrop represents the top uppermost layer of the Jurassic carbonate rock underlying the bauxite horizon (now completely mined out): it is possible to see the regular pattern of fractures and cracks in the limestone strata, filled by bauxite (the carbonate strata are S-dipping). Les Alpilles area: E) Les Baux de Provence – Les Canonnettes: bauxite horizon outcropping on the eastern side of the pit (N-dipping strata). F) Les Baux de Provence – Les Canonnettes, enlargement of (E): detail picture of the upper boundary of the bauxite horizon. The white arrow indicates the polarity of the layer.

tion. Bauxite is massive to oolitic, with rare pisolites and nodules, and shows distinct layers and lamination with bauxitic material intermixed with carbonate clasts. At the Mas de Veirier, the bauxite outcrop has a length of about 200 m and is exposed along the borders of an old pit. The bauxite ore covers the pervasively karstified carbonate footwall. The bauxite body (about 6 m thick) has a regular structure: at the top it is whitish and clayey, whereas at the center it has a massive structure, with minor nodules and pisolites surrounded by a finer matrix. Toward the contact with the carbonate footwall, bauxite presents a brecciated to conglomeratic structure. The most pronounced features of the bauxite horizon are vertical bleaching streaks, which locally give the outcrop a zebra-like appearance (Fig. 5A).

In the Loupian area, the bauxite was sampled in the old open pit of Cambelliès (Fig. 5B). Here bauxite fills the karstified Kimmeridgian limestone in correspondence of a depression, which is considered to be related to *syn*-sedimentary normal faulting (Marchand et al., 2021). The bauxite body is on average 10 m thick and is covered by Late Cretaceous (Maastrichtian) limestone, and by Miocene sedimentary rocks (Marchand et al., 2021). Sampling was conducted on the eastern side of the pit, where bauxite remnants from previous exploitation are still outcropping (Fig. 5C, D). Bauxite infills several karst cavities developed within rounded pinnacles of the underlying karstified limestone. Limestone boulders are diffusely lying within the basal section of the bauxite horizon. At the contact with the overlying limestone, the bauxite body is covered by a clayey horizon (Fig. 5C). The lowermost part of the bauxite horizon has a brecciated matrix-supported structure (Fig. 5E), whereas toward its median part it is dominated by nodular to pisolitic structures; bleaching streaks occur toward the top of the horizon (Fig. 5F).

Near the Bédarieux village, bauxites were sampled in the Carlencas-et-Levas and La Braunhe old mine pits (Fig. 2). In both localities, bauxites overlie Middle Jurassic dolomite (Bathonian; Lajoinie and Laville, 1979) (Fig. 3), and underlie Campanian to early Eocene continental conglomerate (Combes, 1969). It is reported that in Bédarieux, dolo-arenites and shales are intercalated to the bauxite horizon – this suggests two bauxitization events (Combes, 1969), which have been estimated of Early to Late Albian age (Marchand et al., 2021). In the Carlencas-et-Levas old mine pit, bauxite fills deep trenches (up to about 25 m) of the karstified carbonate footwall, which consequently forms high pinnacles within the bauxite bodies. The bauxite body is covered by subhorizontal conglomerate layers (Late Cretaceous) containing bauxite clasts (Fig. 5G), and is cut by a Quaternary mafic dyke (Lajoinie and Laville, 1979). At the contact with the bauxite, the carbonate footwall shows oxidation patches, and is intersected by fractures filled with bauxitic material (Fig. 5H). Here, the bauxite has massive and oolitic textures, and locally includes facies dominated by clasts, nodules, and pisolites embedded in a fine matrix. Other key features include bleaching streaks, as well as subvertical joints with slickensides indicating post-depositional extension. Several samples were collected along a profile roughly perpendicular to the bauxite body on the northern side of the pit, where the lower contact with the footwall is well exposed. The La Braunhe outcrop is quite similar to the latter study area. Only peculiar bauxite facies were sampled here, specifically the massive nodular to pisolitic structure.

A single bauxite locality was investigated in the Saint Chinian-Pierrerue area, along the D134 road, near the Pierrerue village (Fig. 2), where the bauxite horizon is located on Lower Jurassic (Hettangian) dolomite and is covered by Campanian marls (Combes, 1990) (Fig. 3). Here bauxite is clay-rich and shows whitish bleaching streaks at the top. The texture of the bauxite is fine and oolitic, with rare nodules and pisolites in the upper part of the horizon.

4. Material and methods

4.1. Mineralogical and geochemical analysis

The mineralogical and geochemical analyses were performed on 57 samples from Provence (Var and Les Alpilles areas) and 48 from Languedoc (Herault area) bauxite outcrops and old mines (Fig. 2). Multiple samples were collected from key sites (Supplementary data 1), when possible, perpendicularly to the remnants of the various bauxite horizons, from the top to the bottom of the deposits. For several localities where samples were collected along profiles, the whole set of data is shown in Supplementary Fig. 1. This sampling procedure is very effective in detecting potential in-situ (paleo)alteration paths (e.g., Mameli et al., 2007).

Each sample was divided into two halves: the first one was used to prepare polished blocks for optical and scanning electron microscopy equipped with energy-dispersive X-ray spectroscopy (SEM-EDS), whereas the second was milled to carry out whole-rock X-ray powder diffraction (XRPD) and chemical analyses. Blocks were mounted in bi-component epoxy resin (SpeciFix20), polished with diamond suspension (1 μm) and alumina Al_2O_3 (0.3 μm), and carbon-coated prior to SEM analysis.

Qualitative XRPD analyses were performed with a Seifert–GE ID3003 diffractometer, with CuKα radiation, Ni-filtered at 40 kV and 30 mA, 3–80 °2θ range, step scan 0.02°, time 10 s/step at the Dipartimento di Scienze della Terra, dell'Ambiente e delle Risorse (DiSTAR) University of Naples Federico II (Italy). Raw data were treated by the RayfleX (GE) software package. Semi-quantitative XRPD analyses were carried out by using X'Pert PRO diffractometer by PANalytical, at the Istituto Nazionale di Geofisica e Vulcanologia-Osservatorio Vesuviano (Napoli), with a high speed PIXcel detector, Ni-filtered, CuKα radiation, pyrolytic graphite crystal monochromator, at 40 kV and 40 mA in a 3–70° 2θ range with 0.02° steps at 8 s/step. Diffraction patterns were interpreted using the HighScore Plus software and JCPDS PDF-2 database. Mineral abundances were determined on the basis of the whole rock chemical analyses, by using the method of Nyobe (1991).

The micro-textural features and the trace mineralogy were investigated by scanning electron microscopy with energy dispersive spectroscopy (SEM-EDS) by means of a ZEISS EVO LS 15 scanning electron microscope equipped with a X-Max detector (Natural History Museum, London, UK). Analyses were carried out at 20 kV, with a 8.5 mm working distance and with a 3 nA current. A Co standard was used for the instrument calibration.

Whole-rock chemical analyses of major and minor elements were carried out at Bureau Veritas Commodities Canada Ltd. (Vancouver, BC, Canada). The total number of measured elements was 43. Moisture and loss on ignition (LOI) were determined separately at 105 °C and 1000 °C. For major elements analysis, dried samples were mixed with lithium tetraborate/metaborate flux followed by fusion and casting into glass discs, then analyzed by X-ray fluorescence (XRF) (package code: XF701). Rare earth and refractory elements were determined by inductively coupled plasma-mass spectrometry (ICP-MS) following a $LiBO_2/Li_2B_4O_7$ fusion (package code: LF100).

4.2. Multivariate statistical analysis

Multivariate statistical analyses were carried out on whole-rock geochemical data via the R software (v 3.6.1) to draw a comparison between the selected bauxite deposits and to unravel the bauxitization-related geochemical tendencies on the scale of the full dataset. Principal component analysis (PCA) was performed by using the *princomp* and *ggbiplot* packages from the Comprehensive R Archive Network (CRAN). The proportions between variables

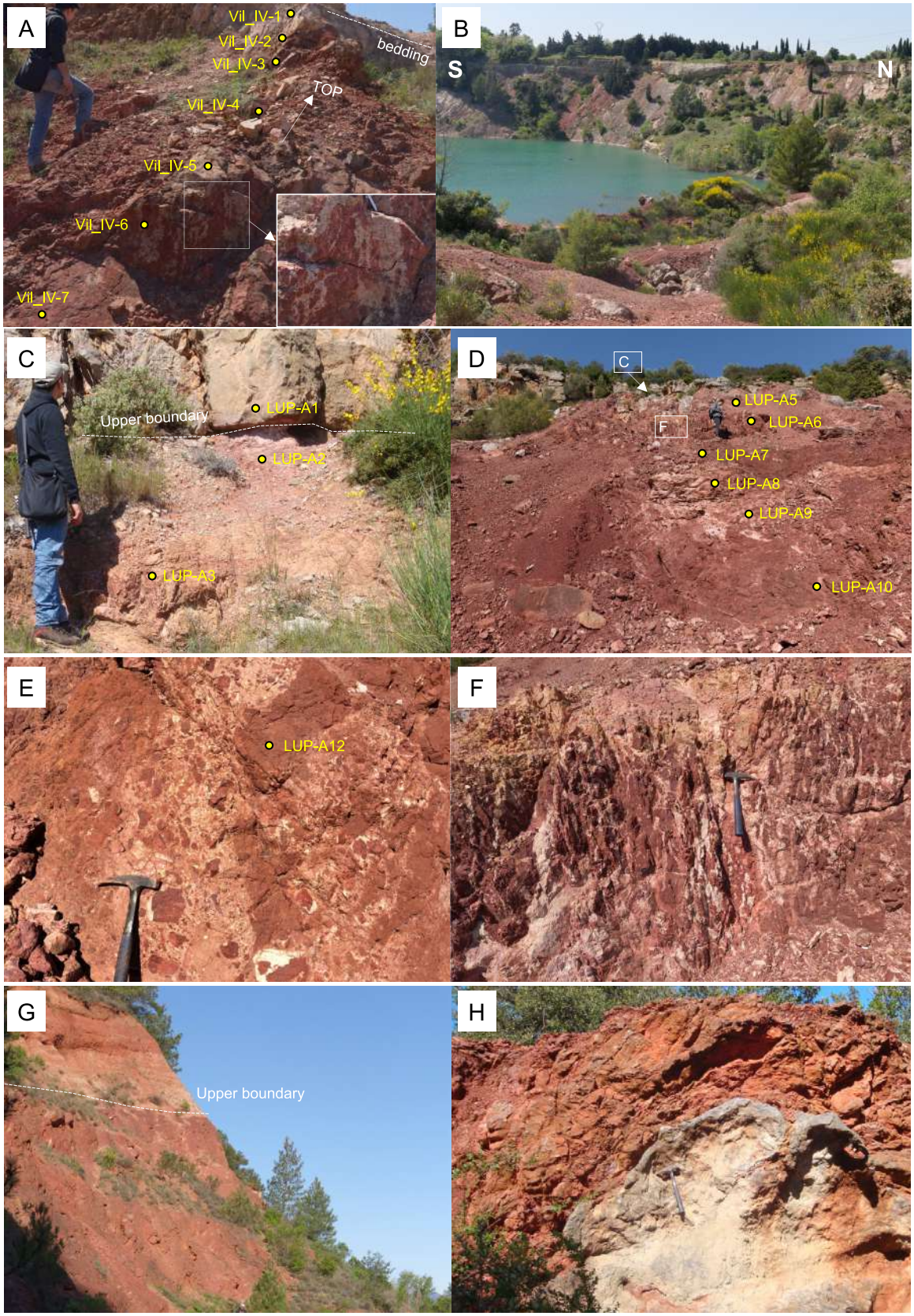

Fig. 5. Examples of bauxite outcrops in Languedoc, with the positions of the collected samples. Herault area: A) Villeveyrac – Mas de Veirier: picture of the sampled bauxite profile, with an enlargement of bleaching streaks occurring within the bauxite horizon. The white arrow indicates the polarity of the layer. B) Loupian – Cambelliès: view of the old pit now filled by a mine lake. In the foreground it is possible to see limestone boulders outcropping in the middle of the bauxite. In the background, the surface of the presumed synsedimentary normal fault is exposed (Marchand et al., 2021). C) Loupian – Cambelliès: clayey material occurring at the upper boundary of the bauxite deposit, below the overlying carbonates. D) Loupian – Cambelliès: main area of sampling, showing the location of the area shown in (C). E) Loupian – Cambelliès: bauxite with a brecciated matrix-supported structure. F) Loupian – Cambelliès, enlargement of (D): bleaching streaks occurring toward the top of the horizon. G) Bédarieux – Carlencas-et-Levas pit: upper section of the bauxite horizon in contact with sub-horizontal conglomerate layers (Late Cretaceous). H) Bédarieux – Carlencas-et-Levas pit: lower contact between the bauxite and the underlying carbonate footwall, showing in-situ alteration.

and observation fulfill the criteria applied to ensure the stability of the PCA output, i.e., n > p2 + 3p + 1, where n is the number of samples and p is the number of variables (Reimann et al., 2011). For this reason, considering the total of 102 whole-rock geochemical analyses, to perform the PCA, we had to reduce the number of elements, i.e., variables, from 43 to 14. The elements used as data input for the statistical analysis were selected both based on their variance and on their significance in bauxite ores. Firstly, considering that the main aim of PCA is dimension reduction, i.e., to find a limited number of components (desirably only two) expressing as much of the inherent variability of the complete data set as possible, thereby promoting the selection of elements characterized by the highest variance (variability) in the database. Secondly, we made sure that the elements with the highest variance were also significant for explaining the mineralizing processes related to deep weathering (see for example, Mongelli et al., 2014, 2016; Torró et al., 2017). According to these criteria, the following oxides and elements have been selected: SiO_2, Al_2O_3, Fe_2O_3, TiO_2, Zr, Ce, V, La, Y, Nb, Ga, Th, Hf and U. Prior to PCA, the data were subjected to a normalization through isometric log ratio transformation. This pre-treatment requires a data matrix with no zero values, therefore, concentrations below the detection limit (dl) have been reported as 0.65*dl (Martín-Fernández et al., 2003). The interpretation of the PCA results has been based solely on the PC accounting for at least 5% of the variance within the dataset. Afterwards, a multivariate analysis of variance (MANOVA test) was performed to test whether the elements used in the PCA produced statistically significant differences occur among the studied bauxite deposits. For the MANOVA computation we relied only on the PC axes cumulatively accounting for at least 95% of the total variance in the dataset. Then we performed a multivariate multiple linear regression between the same PC axes, as dependent variables, and the groups we identified and encoded as dummy independent variables, to feed a post hoc Tukey's test to measure the pairwise differences between groups and to statistically identify which groups cluster together. Factor analysis (FA), performed by the *factanal* function and the Varimax rotation was performed both on the outliers-free data and on the outliers with the aim to recognize interlemental associations and to shed light on the processed leading to anomalous enrichment of critical metals (e.g., REE, Y, Ga, etc.).

4.3. U-Pb dating of zircons

Considering that U-Pb zircon dating was already carried out on the Languedoc bauxites (Marchand et al., 2021), our study has been focused on the Provence deposits (Les Alpilles and Var). Two samples were prepared from the Les Baux de Provence (Les Canonnettes) and Mazaugues (Calas-la Caire) deposits, by mixing bauxite sample material collected perpendicular to the bauxite horizon (Fig. 4A and 4E). The representative samples had weights between 5 and 10 kg per sample. Zircon grains were separated from selected samples using standard heavy mineral separation techniques. Zircons were mounted in 1-inch epoxy disks, polished and imaged through cathodoluminescence (CL) imaging to characterize internal zircon textures. Following CL imaging we used laser ablation inductively coupled plasma mass spectrometry (LA-ICP-MS) at the Department of Earth Sciences of ETH Zurich to determine U-Pb ages. A 193 nm Resonetics Resolution S155 laser ablation system coupled to a Thermo Element XR, Sector-field single collector ICP-MS (Guillong et al., 2014) was used. Laser parameters include a spot size of 30 μm, a repetition rate of 5 Hz and an energy density of ~2.5 J cm^{-2}. The ablation aerosol was mixed in the fast washout S-155 ablation cell (Laurin Technic) with carrier gas consisting of helium (ca. 0.7 L min^{-1}) and make-up gas consisting of argon (ca. 1 L min^{-1}). The ablated aerosol was then homogenized by flushing through a squid device before introduction into the plasma torch. The single collector sector-field MS is equipped with a high-capacity (80 m^3 h^{-1}) interface pump to improve sensitivity. Before each analytical session, the instrument is optimized on NIST SRM612 glass to achieve a detection efficiency in the range of 1% (on Pb, Th, U) while keeping a low oxides production ($^{248}ThO^+$ / $^{232}Th^+ \leq 0.25\%$) and the U/Th intensity ratio of ca. 1. Intensities were recorded for the following isotopes: ^{202}Hg, ^{204}Pb, ^{206}Pb, ^{207}Pb, ^{208}Pb, ^{232}Th, ^{235}U, and ^{238}U. Further information about the instrumental condition is reported in Supplementary Data 2 following the community-derived guidelines (Horstwood et al., 2016).

The GJ-1 standard was used as calibration reference material (CRM). Validating reference materials (VRM) included Plešovice (337 Ma; Sláma et al., 2008) and 91,500 (1065 Ma; Wiedenbeck et al., 1995). The VRMs results show the achievable precision and accuracy of the method, which is in the range of 1%. The data was reduced using the software Iolite 2.5 (Paton et al., 2010; Paton et al., 2011) with VizualAge (Petrus and Kamber, 2012). No common-Pb correction was applied, but integration intervals were set to exclude inclusions, common Pb and unstable parts of the signal. The long-term external uncertainty is in the range of 1.5% for $^{206}Pb/^{238}U$ dates and is composed of the uncertainty from the applied corrections, uncertainty of the decay constants, the uncertainty on the true $^{206}Pb/^{238}U$ ratio of the primary standard GJ-1, and possible uncertainty from matrix effects.

For both our new U-Pb data and for data from the literature, only zircon dates with a concordance level of 95–105% concordance (defined as [$^{206}Pb/^{238}U$ date]/ [$^{207}Pb/^{235}U$ date] × 100) are used for density plots with $^{206}Pb/^{238}U$ dates used for dates younger than 1200 Ma and $^{207}Pb/^{206}Pb$ dates used for older dates.

5. Results

5.1. Mineralogy and petrography

All the sampled bauxites, both in Provence and Languedoc, are mostly boehmitic, and show variable (also high) amounts of kaolinite, and low concentrations of hematite (Supplementary data 1). Anatase is a ubiquitous minor mineral. In the Var area, it is possible to observe an almost similar spatial distribution of boehmite and kaolinite, with the clay fraction (i.e., kaolinite) more abundant either at the top of the bauxite horizon, directly at the contact with the overlying carbonate rock (e.g., Calas-la Caire mine site), or toward the bottom of the sampled profiles (e.g., Combecave – Brignoles site) (Supplementary data 1). These features are observed in the Les Alpilles area as well. In particular, at Les Baux de Provence – Les Canonnettes, where kaolinite has a high concentration both at the top and toward the bottom of the horizon, whereas boehmite prevails at the center (Supplementary data 1). However, all the sampled bauxites from the Les Alpilles district are on average more clayey than in the Var deposits (Supplementary data 1). In the Herault area, the kaolinite-boehmite dichotomy occurs to a lesser extent than in previously mentioned deposits. The Villeveyrac Mas de Veirier bauxite seems to be mineralogically homogeneous. The Loupian deposit is characterized by a central boehmitic horizon, with kaolinitic intervals toward the bottom. The Loupian bauxite is overlaid by a kaolinite-rich layer. In the Bédarieux and Saint Chinian samples kaolinite prevails (Supplementary data 1). In the Les Baux de Provence – Les Canonnettes and Loupian, bauxite directly at the contact with the carbonate bedrock shows a local kaolinite decrease.

The analyzed bauxites are mostly oolitic, with nodules and pisolites in a fine matrix (Fig. 6A, B, D, I, N). Concretions and crusts are common within the samples (Fig. 6B, D, H, I), as well as millimetric

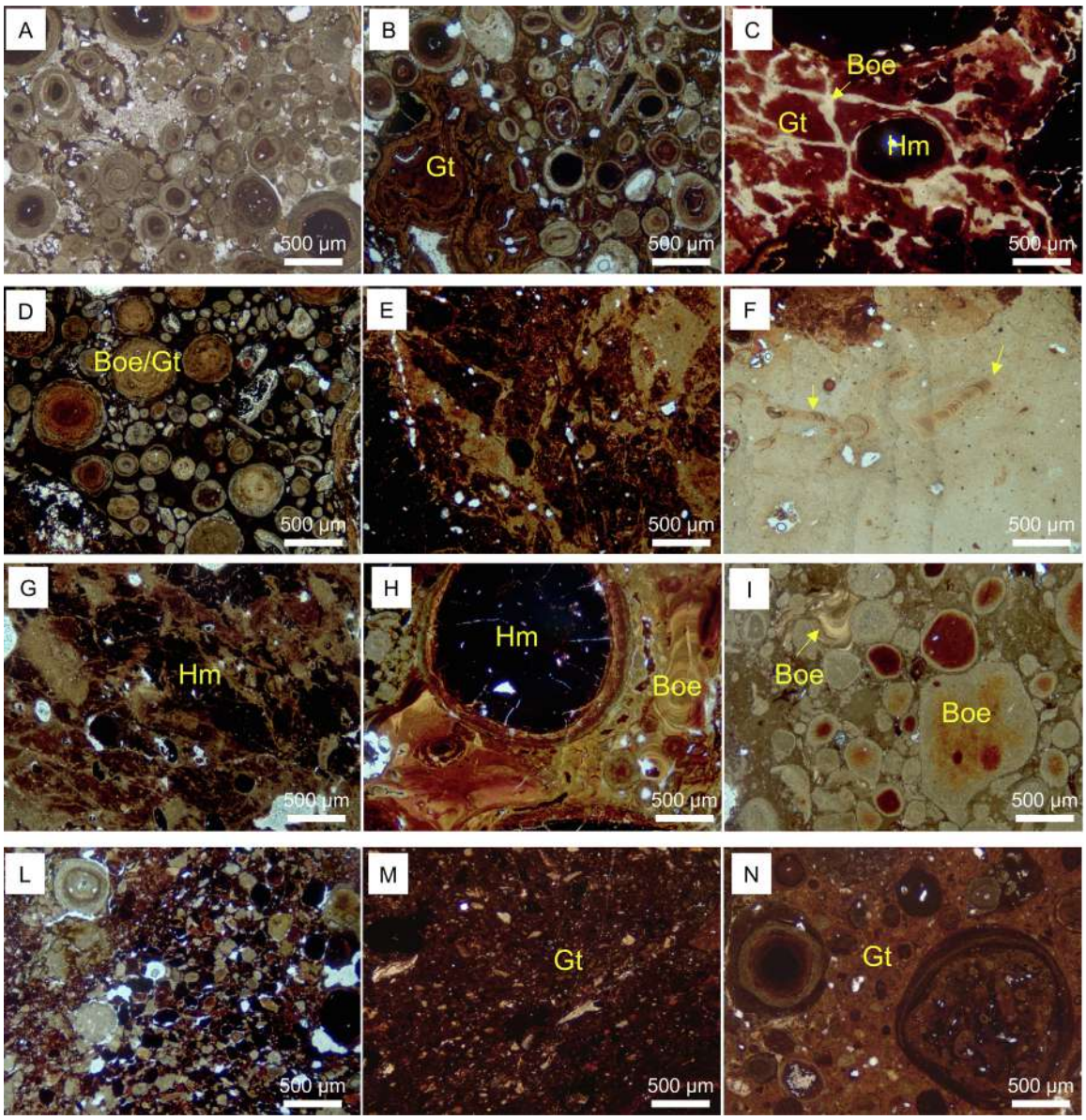

Fig. 6. Summary of textural features identified in the studied deposits. A) MPC6B: oolitic bauxite, with boehmite cement. B) CMB1: oolitic bauxite, with goethite cement. C) CMB4: bleaching structure. D) LBP II 2B: oolitic bauxite, with goethite cement. E) LBP 3: deferrification structures. F) LBP 7: Burrows (highlighted with yellow arrows) filled with Al-rich material. G) VIL IV 3: bleaching structure. H) LUP A3: hematite nodule, surrounded by boehmite cement. I) LUP A9: oolitic bauxite with void-filling concretionary boehmite (yellow arrow). L) LUP A15: detrital layer. M) BC-B2: detrital layer. N) BC-B3: oolitic bauxite.

sub-equant reddish-colored "lump"-shaped textural elements, which at macroscopic scale can be misinterpreted as bauxite clasts, yet they represent relics bleaching streaks (Fig. 6C, E, G). Fragmental oolites and clasts are common, but they are subordinate to the "authigenic" mineral fraction (i.e., clays and hydroxides). Burrows were recognized in the Les Baux de Provence – Les Canonnettes samples. Detrital layers are quite common in the Languedoc bauxites, specifically in Loupian and Bédarieux (Fig. 6L, M).

In oolites and pisolites, boehmite and hematite prevail, whereas kaolinite is mostly concentrated in the matrix of the samples, finely mixed with boehmite. Pisolites and oolites have an Al-hematite or Al-goethite core, rimmed by alternating layers of Al-hematite/Al-goethite and boehmite – that locally can be Fe-bearing. Anatase occurs as discrete mineral grains within the oolitic and matrix fractions. Zircon, monazite, xenotime and rutile are common detrital minerals in all the considered sites (Fig. 7A-E). Authigenic LREE-minerals (e.g., cerianite) have been sporadically detected in the analyzed samples (Fig. 7F).

5.2. Geochemical composition and multivariate statistical analysis

5.2.1. Whole-rock geochemistry

Fig. 8 shows the chemical composition of the studied bauxite deposits (reported in Supplementary data 3, 4 and 5). Among the major oxides Al_2O_3 is the dominant component (avg. = 47.00 wt %), followed by Fe_2O_3, SiO_2 and TiO_2 (avg. = 21.74 wt%, 15.05 wt% and 2.52 wt%, respectively). SiO_2, Al_2O_3 and Fe_2O_3 account for a relevant proportion of the variance within the dataset (i.e., 157.64, 110.31 and 84.78, respectively). Conversely, the variability of TiO_2 is negligible (0.59). However, Fe_2O_3 is the sole major oxide having an outlier (Fig. 8), corresponding to a bauxite sample from the Le Rigoulier profile, which is particularly rich in hematite (LT-

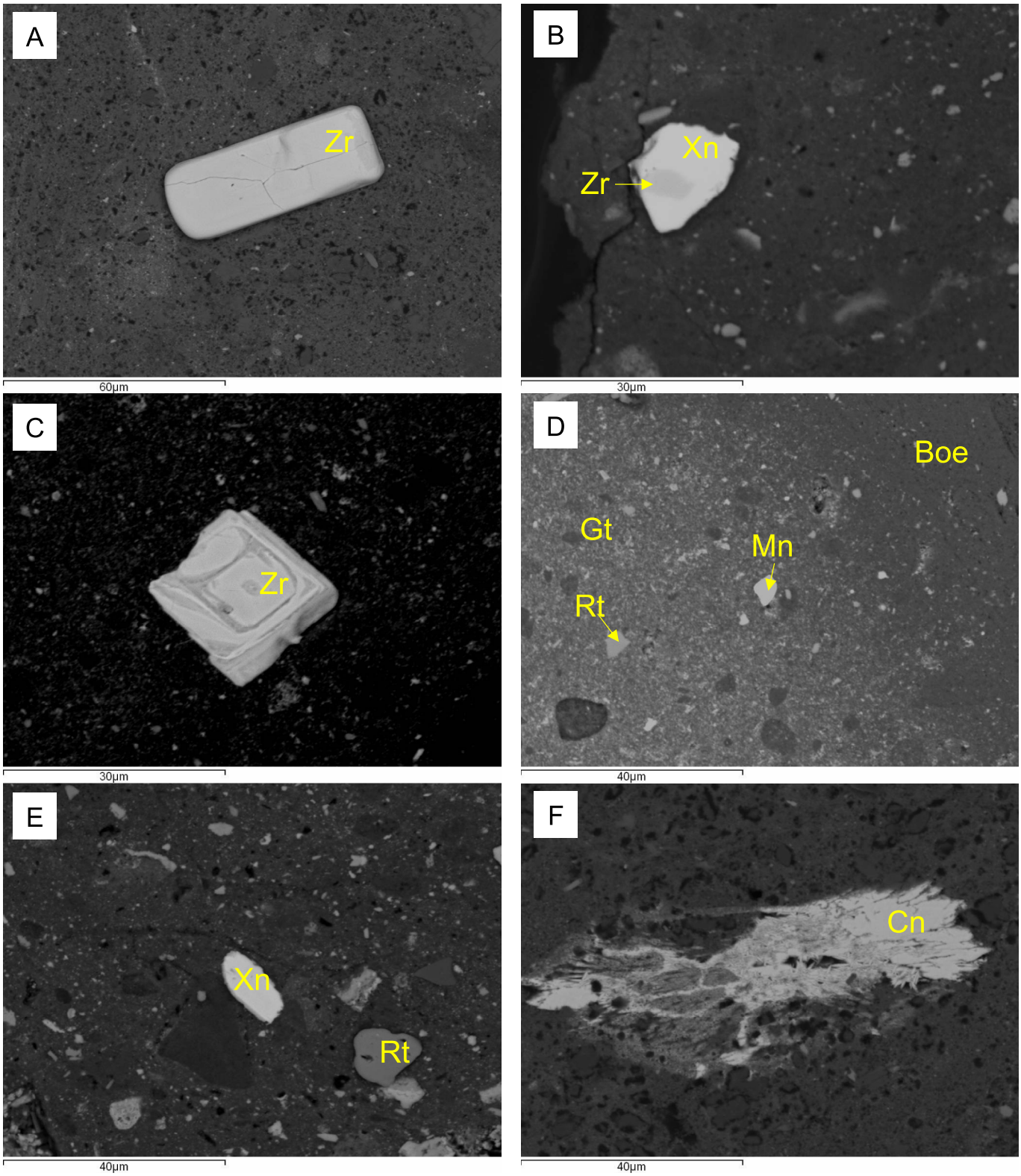

Fig. 7. Textures of significant trace minerals occurring in the bauxites. A) LBP7: zircon grain in boehmite matrix. B) MPC7: xenotime grain with a zircon inclusion. C) MAM1: zoned zircon grain. D) MMT3: monazite and rutile detrital grains in Al-Fe hydroxide (boehmite-goethite matrix). E) CMB2: xenotime and rutile in a mixed matrix. F) LBP4: secondary cerium oxide cerianite.

LR_2). Concerning the key trends for major oxides, Fe_2O_3 and TiO_2 show a normal distribution, while Al_2O_3 and SiO_2 have a bimodal distribution (Fig. 9). In this frame, Al_2O_3 and SiO_2 have no outliers although their distribution is characterized by anomalous concentrations. Specifically, a significant portion of the dataset shows Al_2O_3 concentrations <40 wt% and SiO_2 >25 wt% (Fig. 9).

The detected trace elements can be subdivided in three groups: i) high field strength elements, i.e., Zr, Nb, Th and Hf (avg. = 786

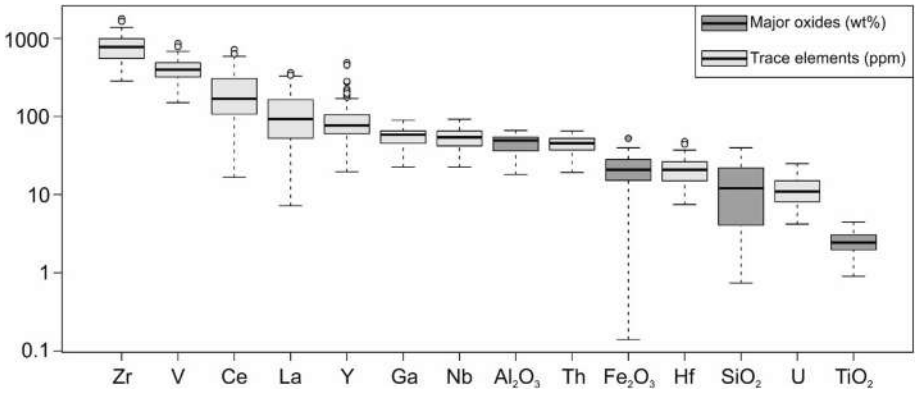

Fig. 8. Box and whisker plots showing the distribution of normal distributed data and of outliers within the geochemical dataset. Note: along the y-axis, major oxides are reported in wt.%, whereas minor and trace elements are reported in ppm.

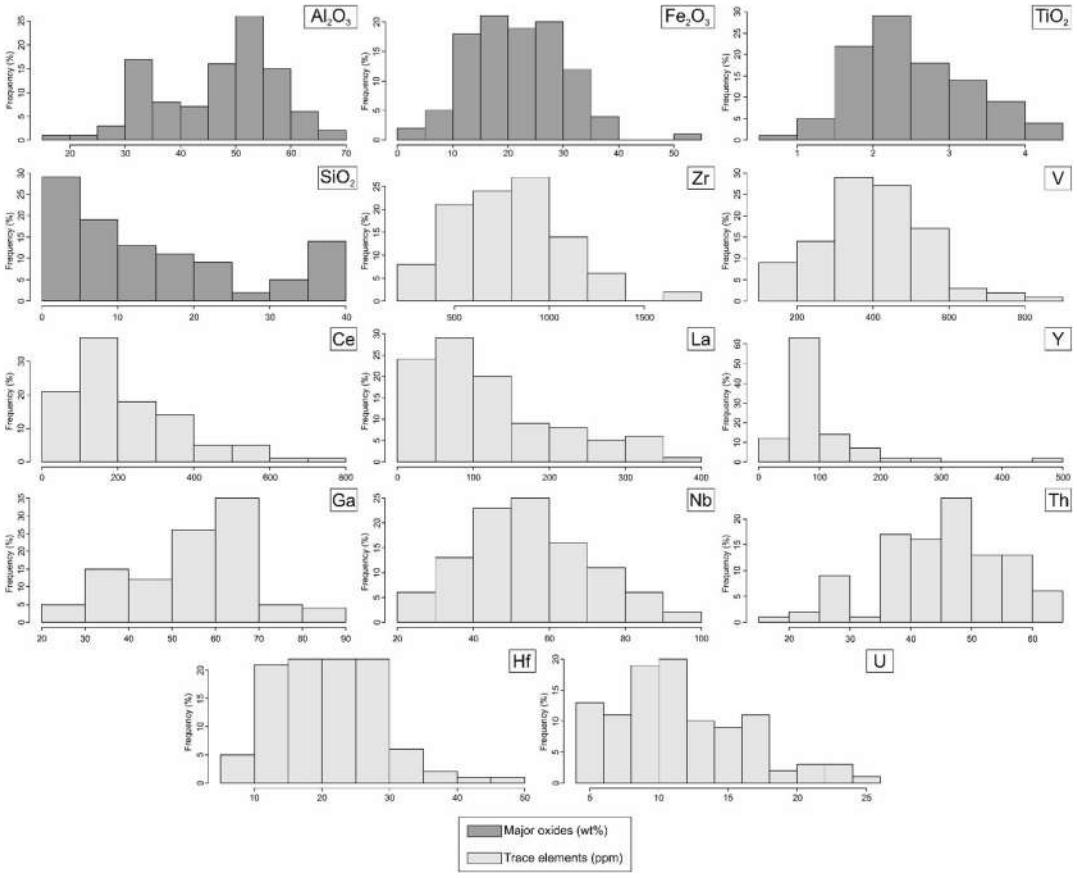

Fig. 9. Histograms showing the data distribution of major oxides, as well as minor and trace elements, within the geochemical dataset.

ppm, 54 ppm, 45 ppm and 21 ppm, respectively); ii) transition metals, i.e., V (avg. = 405 ppm); iii) critical metals, i.e., Ce, La, Y and Ga (217 ppm, 120 ppm, 96 ppm and 55 ppm, respectively). Zirconium, V, Ce, La, Y, Nb and Ga have a remarkable variance (82824, 23169, 18837, 8270, 5083, 253 and 201 respectively), while the variability of Th, Hf and U (102, 58 and 21, respectively) is less relevant. Among trace elements, Zr, V, Ce, La, Y and Hf show several outliers exceeding the 95th percentile (Fig. 8). All the trace elements, except for Th, show a normal distribution of data (Fig. 9).

The distribution of the major elements along the bauxite profiles reflects the described mineralogical changes in the studies districts (Supplementary Fig. 1): e.g., SiO_2 is most abundant when kaolinite increases, whereas Al_2O_3 prevails in correspondence of boehmitic horizons. Conversely, trace elements do not show such obvious distributions, whereas regular trends can be followed looking at the values of the ratios Eu/Eu* and Ce/Ce* (Supplementary Fig. 1). The Eu/Eu* index shows no significant fluctuation along the analyzed profiles (avg. Eu/Eu* is 0.62 for the Var bauxites, 0.61

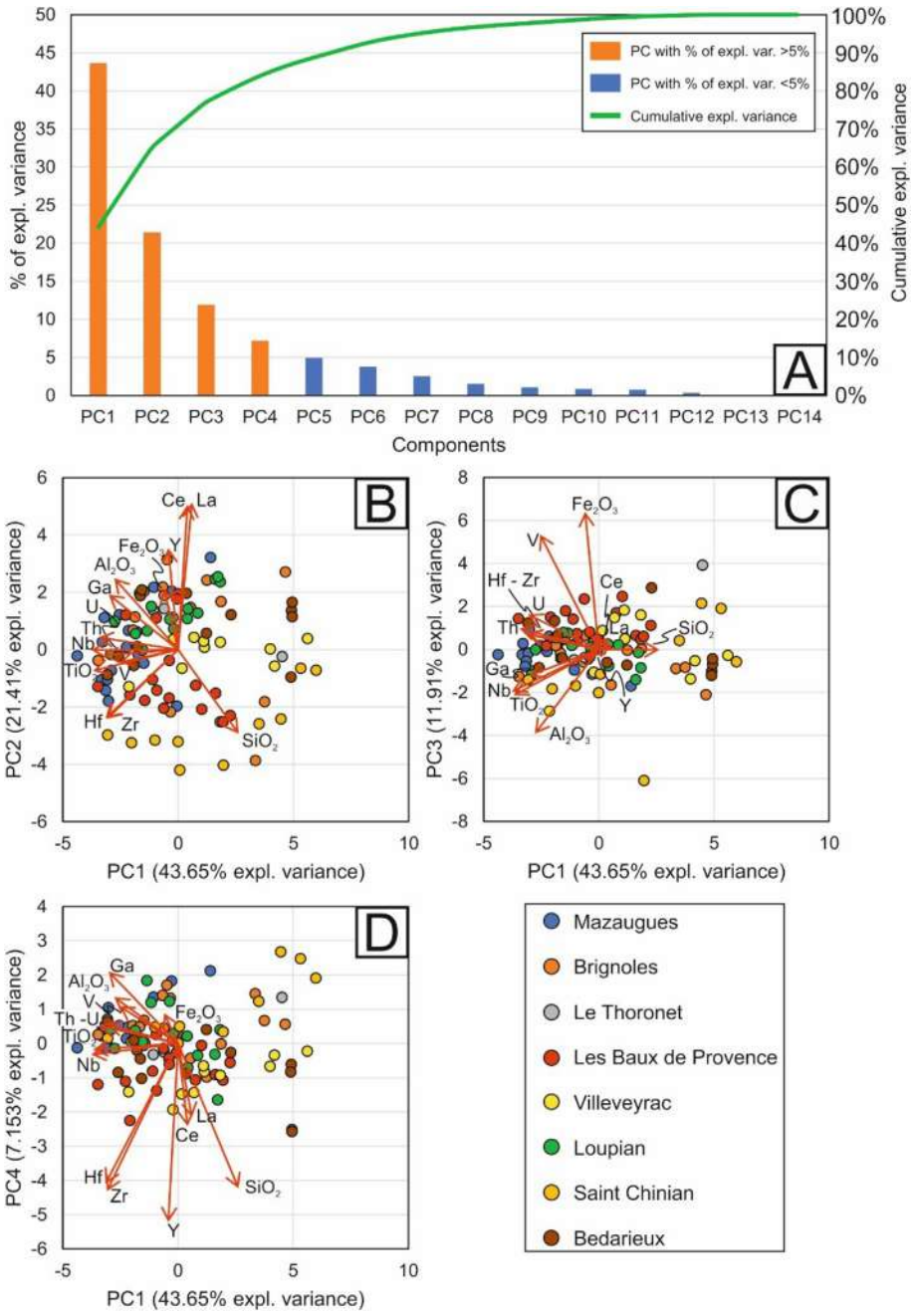

Fig. 10. Results of the principal component analysis (PCA). A) Scree plot showing the % of explained variance of each PC of the dataset; B), C) and D) PC1 versus PCn biplots.

for the Les Alpilles, and 0.62 for the Languedoc deposits), whereas Ce/Ce* often increases from the bottom toward the top of certain bauxite horizons (e.g., from 0.51 to 1.91 at Loupian), although not reaching extremely high values or following very straight trends (Supplementary Fig. 1).

5.2.2. Multivariate statistical analysis

Principal component analysis on whole-rock geochemical data has shown that the first four components (PC1 to PC4), exceeding the variance cut-off value of 5%, account for 87% of the explained variance in the dataset (Supplementary data 6 and Fig. 10A). The relationship between the PC1 and the PC2 is shown in Fig. 10B. The PC1 (43.65% explained variance) produces the most significant clustering between the selected bauxite deposits. The most relevant aspect visible in the PC1 vs PC2 projection is the anticorrelation between the SiO_2 eigenvector, having positive PC1 values, and the TiO_2-V-Nb-Th-U group, which has negative PC1 values. Similarly, the Hf-Zr and the Al_2O_3-Ga pairs have negative PC1 values, although the direction of the eigenvectors in the PC1 – PC2 dimension is also controlled by the PC2. In particular, the Hf-Zr pair has negative PC2, conversely, the Al_2O_3-Ga pair has positive PC2. In this frame, Fe_2O_3, Y, Ce and La form a group having positive PC2 values and a negligible contribution of the PC1. Data distribution controlled from clustering effect of the SiO_2 vs TiO_2-V-Nb-Th-U dichotomy belongs mostly to the Villeveyrac, Saint Chinian, Le Thoronet, Bedarieux and part of the Les Baux de Provence bauxites and form a linear trend along the PC1. The Mazaugues and Brignoles analyses form a trend stretching from the 3rd to the 4th quadrant and thus show a high degree of correlation with the Hf-Zr, TiO_2-V-Nb-Th, Al_2O_3-Ga and Fe_2O_3-Y-Ce-La groups. Samples from Loupian, as well as a few of those from Les Baux de Provence,

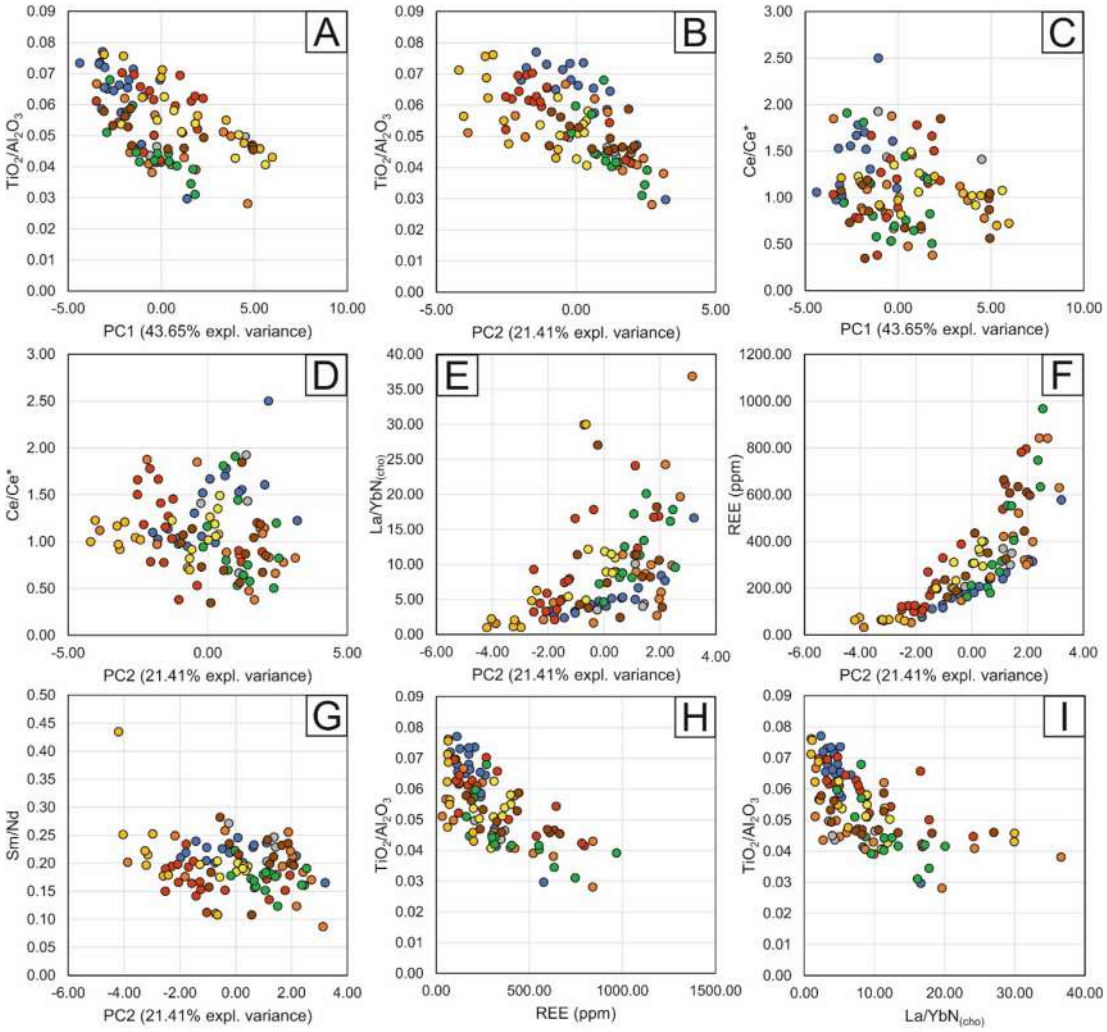

Fig. 11. Correlation diagrams: A) to G) Binary plots showing the relationships between selected PC and the most significant chemical indexes used for bauxites deposits (i.e., TiO_2/Al_2O_3, Ce/Ce* and $La/Yb_{N(cho)}$), as well as with the REE concentration. H) and I) TiO_2/Al_2O_3 vs REE and TiO_2/Al_2O_3 vs $La/Yb_{N(cho)}$ plots showing the relationship between the weathering degree and the lanthanides enrichment. For legend colors refer to Fig. 10.

are located in the 4th quadrant and are correlated with the TiO_2-V-Nb-Th, Al_2O_3- Ga and Fe_2O_3-Y-Ce-La groups.

The results of the MANOVA test (Pillai = 2.492; Approximate F = 7.4235; *p*-value = 0.5252) performed on the PC1 to PC7 (cumulatively accounting for 95.36% of the variance, Fig. 10A and Supplementary data 7) show that no statistically significant differences occur between the studied bauxite deposits besides the clustering of data observed mainly in the PC1 vs PC2 projection.

Plots involving the PC1 and PC2 scores and several geochemical indexes traditionally used to track bauxitization processes, as well as the total REE contents are shown in Fig. 11A to 11G. The PC1 and PC2 form a well-fitting negative trend with the TiO_2/Al_2O_3 ratio (Fig. 11A and B), while no clear relationships are visible with the Ce/Ce* index (Fig. 11C and D). The PC2 is strongly correlated with the $La/Yb_{N(cho)}$ index and with the total REE concentration (Fig. 11E and F). Furthermore, a slight negative correlation is also visible between the PC2 and the Sm/Nd ratio (Fig. 11G). In the studied bauxites the TiO_2/Al_2O_3 ratio shows a conspicuous variability (from ~0.03 to ~0.08) and is anticorrelated with both the REE contents and with $La/Yb_{N(cho)}$ proxy (Fig. 11H and I).

The results of the FA carried out on the normal-distributed geochemical data are shown in Supplementary data 8. Four factors collectively account for 77.70% of the variance within the dataset. The first factor (36.90% explained variance) shows positive weightings for Al_2O_3, Ga, TiO_2, Nb, Th, U, Y, whereas it shows negative weightings for SiO_2. The second factor (15.80% explained variance) includes high positive weightings of Zr and Hf. In the third factor (13.80% explained variance) Fe_2O_3 and V show positive weightings, while SiO_2 has a negative weighting. In the fourth factor (11% explained variance) Ce and La have both positive weightings. The FA performed on the outliers (Supplementary data 9) shows that four factors account for 79.30% of the data variability. The first factor (21.20% explained variance) shows positive weightings for Zr, V, Hf, U, and TiO_2. Cerium shows a negative weighting in the first factor. The second factor (20.80% explained variance) shows negative weightings for Y and SiO_2 and positive weightings for Al_2O_3, Ga and Nb. The third factor (19.80% explained variance) highlights the dichotomy between the enrichment of lanthanides (i.e., Ce and La) and transition metals (i.e., Al_2O_3, Fe_2O_3 and V). The fourth factor (17.50% explained variance) shows positive weightings for Al_2O_3, TiO_2 and Ga.

5.3. U-Pb zircon dating

Detrital U-Pb zircon dating was carried out on the Les Baux de Provence (Les Canonnettes) and Mazaugues (Calas-la Caire) bauxites (Fig. 12; Supplementary data 10). Catholuminescence images of zircons from Les Baux and Mazaugues show that the population is very heterogeneous, typical of detrital samples (Supplementary

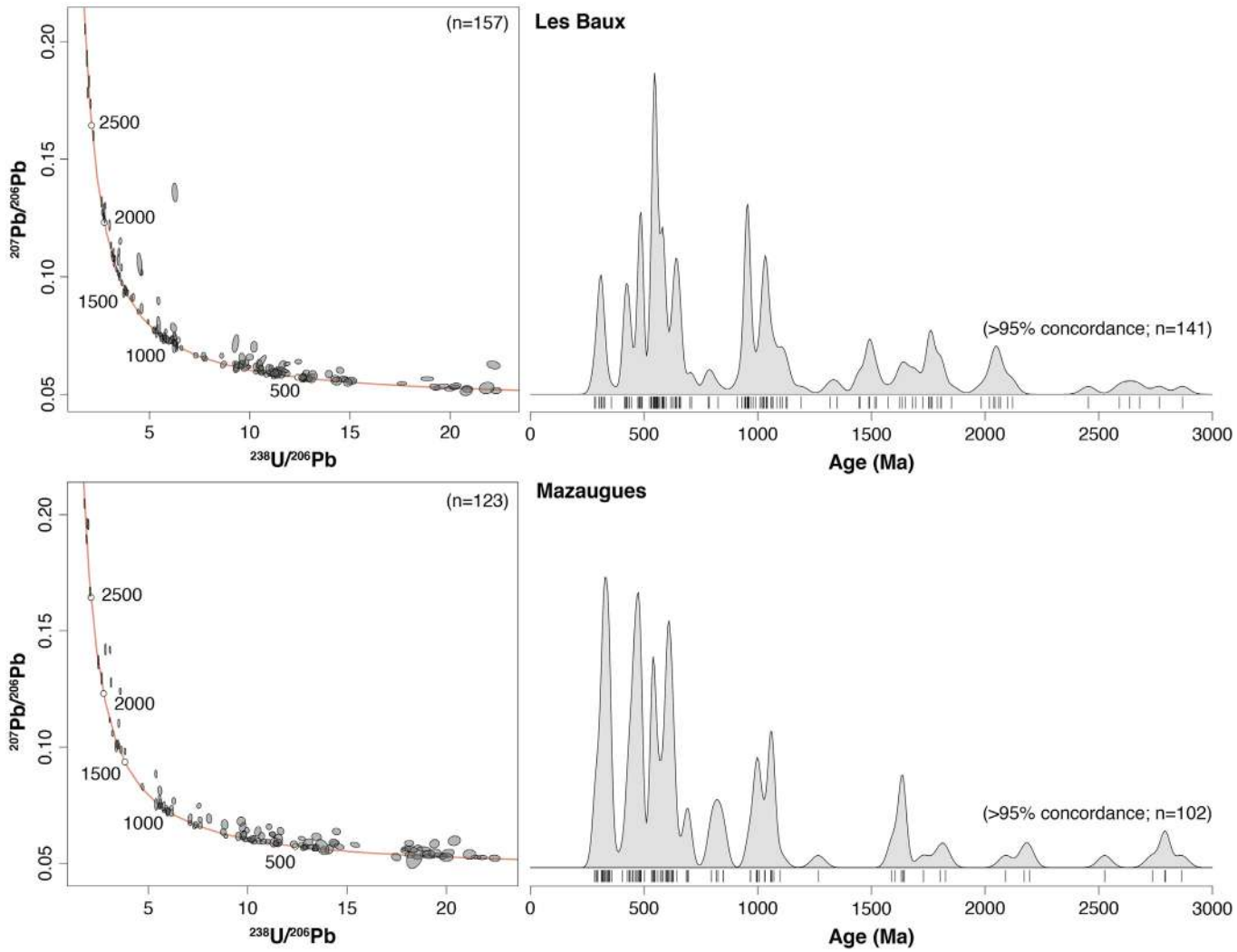

Fig. 12. LA-ICPMS zircon U-Pb dating results of the bauxite samples. Left column presents the Tera-Wasserburg diagrams. Right column presents the ranked $^{206}Pb/^{238}U$ dates of concordant analyses and the corresponding density plots. All uncertainties are given at 95 % confidence (2σ).

material 1 and 2). The selected samples feature an extensive and complex record of mostly concordant U-Pb dates ranging from the Archean to the Carboniferous (Fig. 12). While samples share a similar pre-Rhyacian signature (ca. 8% of the dates), they display a distinct 1.3–2.0 Ga record with Mazaugues showing a minor peak around 2.6 Ga (19% of the dates) and Les Baux showing a protracted record with sub-peaks at 1.35, 1.50, 1.65, and 1.75 Ga (19% of the dates). At Mazaugues, the Stenian-Tonian population (20% of the dates) shows peaks at 0.82, 1.00 and 1.06 Ga, while that at Les Baux (25% of the dates) peaks at 0.80, 0.95, 1.03, and 1.10 Ga. Both locations have a dominant Ordovician to Cryogenian zircon population (~43% of the dates) with distinct peaks: at Mazaugues, this population is characterized by three sub-equal age peaks at 470, 545 and 610 Ma; conversely, Les Baux features a dominant peak at 550 Ma and four secondary ones at 425, 480, 580 and 640 Ma. Finally, Variscan-aged zircon are centered on 330 Ma at Mazaugues and 310 Ma at les Baux.

6. Discussion

6.1. Genetic processes

The new data presented here are in agreement, at the outcrop scale, with geological and mineralogical features reported in previous works (e.g., Lajoinie and Laville, 1979; Combes, 1990: Marchand et al., 2021). As reported by other authors (e.g., Lajoinie and Laville, 1979; Guendon and Parron, 1985), the Mazaugues – Calas-la Caire, Combecave – Brignoles, Les Baux de Provence – Les Canonnettes outcrops are characterized by quite regular mineralogical distribution, with prevailing amounts of kaolinite at the top or at the bottom of the bauxite bodies, and major amounts of Al-hydroxides at the core of the mineralized horizons. For these sites, these regular mineral variations are interpreted to be related to in-situ weathering processes overprinted to, or associated with, local sedimentary reworking. For the France bauxites, these features echo the so-called *parallochthonous* and *parautochthonous* models of Combes (1990). These models allow to reconcile the occurrence in the bauxite layers of certain sedimentological features (e.g., the presence of broken clasts and detrital layers), with local mineral zonation almost resembling the more distinct stratigraphy of the lateritic bauxites (see, Freyssinet et al., 2005), which derive from differential element leaching resulting from in-situ weathering (Freyssinet et al., 2005). For the Languedoc bauxites, and specifically for the Villeveyrac basin, Marchand (2019) and Chanvry et al. (2020) propose a pure allochthonous model evidencing the occurrence of first-order textural features compatible with mass-flow to debris-flow sedimentary processes. The conjunct occurrence of kaolinite at the top of the bauxite hori-

zon was interpreted as the result of the erosion of an autochthonous laterite cover in the upstream drainage, which led to a reverse stacking of the reworked autochthonous lateritic profile in the depositional basin. Although we agree on the possible pure sedimentary nature of several sections of the Languedoc bauxite profiles, the reverse staking model is, in our opinion, unlikely. To support this statement, it could be considered the world class lateritic bauxite district of the Guyana shield (e.g., Monsels and van Bergen, 2017, 2019). This district comprises the "coastal-plain bauxites", formed on sedimentary parent material in the coastal lowlands, and the "plateau bauxites" largely originated from weathering of the Proterozoic basement. Although the coastal-plain bauxites show lithofacies complexity and sedimentary features related to bauxite reworking in an alluvial to fluvial environment, the occurrence of reverse staking profiles is very rare. In a few cases in the Paranam-Onverdacht-Lelydorp bauxite district (Suriname), the increase of kaolinite towards the top of the weathering profiles was interpreted to result from the kaolinitization of the bauxite (in-situ SiO_2 source) or resilication (external SiO_2 origin), which was also been reported for other local deposits as well as for Brazilian bauxites (e.g., Monsels and van Bergen, 2017, 2019). Following these similar cases, we suggest that the kaolinite increase toward the top of the bauxite horizons (i.e., Les Baux de Provence, Mazaugues) can also be associated with late re-silicification processes (Dangić, 1985, 1988; Lucas, 1989; Freyssinet et al., 2005). Therefore, while the sedimentary nature of the kaolinite-rich clayey material occurring at the top of Villeveyrac bauxites is a possibility, we are more favorable to its derivation from secondary weathering of clay sediments deposited above the bauxites. This interpretation is later discussed against the geochemical data.

Bleaching streaks were documented in several investigated outcrops. These features are commonly related to in-situ iron leaching due to the establishment of low pH and low Eh conditions in the groundwaters (Norton, 1973). These conditions are peculiar of continental to transitional environments, characterized by organic matter degradation, such as tropical soils (Norton, 1973). Such conditions have been identified in the Greek karst bauxites (Kalaitzidis et al., 2010), where the bleaching streaks are associated with coal-lignite layers lying above the bauxite horizons. Through investigations of the coal layers, it was suggested that the alteration developed in a paralic sedimentary environment (lagoon to delta) characterized by rheotrophic, high groundwater-table (lacustrine) conditions for the peat-forming stage. In this case, acidic fluids able to leach iron from the underlying bauxite layers were produced by the degradation of pyrite. For the Villeveyrac deposits, Marchand (2019) described two deferrification types: a first post-depositional deferrification, which decreases towards the base of the bauxite horizon and a late fracture-controlled deferrification, which instead is later and extends deeper within the horizons. The former was related to conditions similar to those documented for the Greek bauxites, whereas the latter was associated to percolation of groundwaters in fractures formed during the Oligocene extensional tectonics (Marchand, 2019).

Discussing in detail the textures of the bauxites, the oolitic structure in all the deposits, the presence of several grains/pebbles, and the presence of concretionary bands of hematite>Al-hematite>Fe-boehmite>boehmite were likely formed via in-situ accretion processes (Mongelli and Acquafredda, 1999; Taylor and Eggleton, 2008). The establishment of a weathering profile could be also supported by the presence of tubular burrows, identified, for example, in the Les Baux de Provence profile. Pisolites and oolites can form in the upper mottled zone of the weathering profile, where reworking of the clays decomposes the matrix into microscopic clay pods with or without Fe-oxides (Taylor and Eggleton, 2008), becoming the nuclei of the pisolites, which form concretions through a centripetal evolution (Tardy and Nahon, 1985). Complex and large pisolites/oolites form because of a progressive accretion of cortices around the original cores. This process produces a peculiar texture characterized by distinct pisolites and grains floating in a uniform matrix (Taylor and Eggleton, 2008). The presence of Al-hydroxide concretions agrees with in-situ precipitation of Al-gel. However, as pisolites represent phases with high hardness in a bauxite body, when the deposit is eroded and reworked, they behave as resistant elements, surviving to transport better than softer textural elements. For this reason, in several localities (e.g., Bédarieux, Loupian), the abundance of pisolites, arranged in sedimentary structures (e.g., like cross lamination), suggests and supports the presence of layers composed of reworked bauxite material.

The high abundance of dehydrated or partially dehydrated minerals (boehmite and hematite) in the investigated deposits might be related to: 1) the maturity of the profiles, and/or 2) a low water activity at the time of bauxite formation (Bárdossy, 1982; Tardy and Nahon, 1985). Support for the first hypothesis is given by the Mesozoic age and the certain burial degree of France bauxites, in analogy to other Cretaceous bauxites of the Mediterranean realm (Bárdossy, 1982). The second possibility is supported by the karstic nature of the deposits themselves: in fact, it has been suggested that Mediterranean bauxites are more dehydrated than other similar deposits, because they formed in a pedogenic water-unsaturated environment, produced either by the presence of underlying high-weathered and permeable carbonate platform rocks, or by the paleoclimate environment, which was punctuated by dry spells at the time of bauxite formation (Mongelli and Acquafredda, 1999). The peculiar hydrological conditions, characterized by the presence of underlying highly permeable carbonate rocks, could also have favored the leaching of silica from the very lower part of the bauxite horizons, directly at the contact with the bedrock (e.g., in the Les Baux de Provence deposit).

The bulk rock geochemistry is in line with mineralogical and petrographic observations and supports the influence of in-situ alteration in many of the considered deposits. In certain deposits, like Les Baux de Provence, it is possible to clearly detect several proxies indicating in-situ alteration. Beyond the major elements, which follow the trends already described for the main mineral components, the most relevant proxy is represented by the regular distribution of the Ce/Ce* and Eu/Eu* ratios along the bauxite profile (e.g., Mongelli et al., 2014; Supplementary Fig. 1). As reported by several authors (e.g., Mongelli, 1997; Laskou and Andreou, 2003; Maksimović and Pantó, 1996; Mameli et al., 2007; Mondillo et al., 2011; Boni et al., 2013; Mongelli et al., 2014), during the supergene alteration process, Ce behavior deviates from that of the other REEs, because in a oxidizing environment it acquires the Ce^{4+} valence state (from Ce^{3+}), and can be thus precipitated in Ce^{4+}-oxides or be incorporated into Fe-hydroxides, whilst the other REEs remain in solution in the trivalent form (Maksimović and Roaldset, 1976; Koicki et al., 1980; Maksimović et al., 1993; Mondillo et al., 2019). As in a lateritic profile characterized by a stable groundwater, an oxidizing environment is established above the water table, whilst a reducing environment occurs in the phreatic zone, Ce oxidation occurs at the top of the bauxite horizon if the rock is affected by in-situ weathering. Continuous percolation of waters toward the water table will favor Ce fractionation, progressively removing the other REEs, which migrate toward the bottom of the soil. This process is reflected in the geochemistry of the final bauxite horizon, which will develop a positive Ce anomaly at the top. At the same time, the Eu/Eu* ratio remains roughly constant. This happens because Eu is largely unaffected by fractionation during bauxitization (Mongelli et al., 2014). The occurrence of multiple positive anomalies of the Ce/Ce* ratio is commonly interpreted as a marker for periodical fluctuations of

the groundwater table in an overall rising trend (Mongelli et al., 2014). The rough increase of Ce/Ce* ratio toward the top of the horizons, with local positive spikes, is clearly visible in the Les Baux de Provence, Loupian and San Chinian profile (Supplementary Fig. 1). Interestingly, in the Loupian profile, the Ce/Ce* ratio detected in the topmost kaolinite horizon (sample LUP-A2) is lower than the underlying bauxite (LUP-A3 and LUP-4). This feature supports the idea that the mentioned kaolinite horizon has a distinct origin. The Ce/Ce* ratio of the Les Baux de Provence profile roughly increasing toward the top of the bauxite horizon indicates the occurrence of in-situ weathering.

Distinct REE concentrations also show regular distributions along the considered profiles (Supplementary Fig. 1), which can reflect the mentioned processes – the absence of very straight trends is due to two main reasons: 1) the in-situ alteration is overprinted to/by sedimentary reworking; 2) straight trends are uncommon also in lateritic bauxites (see Monsels and van Bergen, 2019). In the Les Baux de Provence profile, the total REE concentration is higher at the center of the deposit, similar to that of Al_2O_3 (Supplementary Fig. 1). This distribution fits well with the documented REE incorporation in Al-hydroxides, with exception of Ce (Mondillo et al., 2019). The Loupian profile is quite interesting because REE concentrations roughly increase toward the bottom of the profile with maximum amounts in the sample LUP-A14 (the deeper sample LUP-A15 is clearly affected by sedimentary reworking; see Fig. 6L). This scheme agrees with a *per descensum* model and progressive REE in-situ leaching toward the bottom of the bauxite profile, also considering the element deportment previously depicted, with REE incorporation in Al-hydroxides, with exception of Ce (Mondillo et al., 2019).

The PCA of the bulk rock geochemistry suggests that the investigated bauxite outcrops are roughly similar to each other (i.e., represent a homogenous population). In fact, the considered deposits do not cluster singularly in the various score plots, but their scores are commonly overlapped. This suggestion is also confirmed by the Tukey's HSD test, which classifies all the deposits in a single group, not evidencing statistical differences between the geochemistry of the considered deposits. Explanations of this statistical feature can be found in a homogeneous nature of the bauxite protores, or in the nature of the bauxitization process itself (Freyssinet et al., 2005), which was so extremely developed to have removed any significant geochemical diversity originally existing between the various analyzed deposits. Going into the detail of the PCA, the PC1 positive scores represent SiO_2-rich bauxite samples (clay-rich zones within the bauxite profiles), whereas negative PC1 scores are TiO_2-rich analyses. Considering that the Si and Ti are decoupled during in-situ weathering processes (Si mobility$\gg>\gg$Ti mobility), the observed variations of PC1 are controlled by the amount of weathering, which affected the diverse bauxite samples and profiles. This relationship (positive correlation between Al_2O_3 and TiO_2, negative correlations between the former oxides and Fe_2O_3 and SiO_2) was also documented by the PCA on major elements only, conducted by Marchand (2019) on hundreds drillcore data deriving from the Villeveyrac bauxite basin. The positive PC2 values indicate ferralitic weathering, which at the scale of the whole dataset is associated with the endowment of lanthanides in the studied ores (see Mondillo et al., 2019). This is confirmed by the positive correlation between Fe_2O_3 and La+Ce, and by the well-fitting positive relationships between the PC2 scores and REE and $La/Yb_{N(cho)}$. Negative PC2 are likely controlled by relevant detrital components, like zircons. In the PC1 vs. PC2 plot, Al_2O_3 is positively correlated with Fe_2O_3 along PC2, and negatively correlated with SiO_2 along PC1, evidencing the first-order processes occurring during bauxitization and mentioned before, that is, the fractionation between silica and more immobile elements (PC1), and the ferralitic weathering (PC2). In the PC1, Ti is commonly associated with HFSE elements (e.g., Nb), which could possibly indicate that newly-formed Ti-oxides (anatase) act as scavengers for trace elements. These correlations are largely expected in the bauxite system (Freyssinet et al., 2005). Gallium, a common by-product of bauxite mining, is perfectly correlated with Al_2O_3 in the PC1 vs. PC2 plot, confirming its association with Al-hydroxides (Mondillo et al., 2019). The PC3 being controlled by the anticorrelation between Al_2O_3 and Fe_2O_3, evidences the second-order processes occurring during the bauxitization, with the development of ferricrete horizons overlying the mottled and plasmic zones (Freyssinet et al., 2005). The PC4, with the negative correlation of La+Ce+Y+Zr+Hf and Al_2O_3+Ga, highlights the third-order control exerted, respectively, by the detrital and the authigenic components occurring in the bauxite deposit. In particular, the statistical association of La, Ce and Y together with Zr and Hf is an indication of the occurrence of detrital REE-bearing minerals, like monazite and xenotime, in association with zircons (which deport Zr and Hf). It must be remembered that the 1st Factor of FA shows the anticorrelation between Zr-V-Hf-U-Ti (positive weightings) and Ce (negative weighting). Therefore, a significant part of the Ce variance indicates a decoupling between this element and Zr-Hf, which is related to the natural separation of Ce from other elements plus REEs during in-situ chemical weathering.

In most bauxite deposits worldwide, Al_2O_3 and TiO_2 are positively correlated due to their similar behavior during bauxitization (Norton, 1973; MacLean et al., 1997; Mondillo et al., 2022). For this reason, in several studies (e.g., Mameli et al., 2007) it was assumed that the TiO_2/Al_2O_3 ratio could be preserved during weathering. However, bauxites of SE France show variable TiO_2/Al_2O_3 ratios at a deposit- to district scale. The relationships between this ratio and other geochemical proxies (e.g., PC1, PC2, REE and $La/Yb_{N(cho)}$) provide some useful insights into this observation. Firstly, the TiO_2/Al_2O_3 is anticorrelated with both PC1 and PC2. The anticorrelation with PC1 can be explained by considering that the Ti mobility is lower than that of Al, thus high TiO_2/Al_2O_3 ratios indicate higher weathering degrees. Therefore, the anticorrelation between TiO_2/Al_2O_3 and the PC2 (as well as with $La/Yb_{N(cho)}$ and REE) would point out that the REE enrichment in association with the formation of Fe-oxy-hydroxides is not favored by high weathering degrees. Note that the absence of correlation between the PC2 and the Ce/Ce* proxy would suggest that in the analyzed samples, the fractionation between Ce and the other REEs (through the formation of Ce^{4+}-bearing new-formed phases) is not statistically significant.

Considering the above points, the factor analysis offers additional clues to shed light on the REE deportment. In the FA performed on normal distributed data, the most important factor (F1) shows a typical bauxitization-related footprint, with positive weightings for elements enriched during the formation of Al-hydroxides (i.e., Ga and Al_2O_3) and Ti-oxides (i.e., Nb, Th, U and TiO_2) and Y, versus negative weightings for SiO_2. In this frame, elements indicating the detrital component (e.g., Zr) occur in a subordinate factor (F2), while lanthanides occur in the F4, wherein very low positive Al_2O_3 and Fe_2O_3 weighting occur (not shown in Supplementary data 8 because they are lower than the 0.4 cut-off values). This confirms that in the n-distributed data, the REE deportment is controlled by the scavenging effect exerted by oxy-hydroxides (Mongelli and Acquafredda, 1999; Mondillo et al., 2019). However, as mentioned in the data description, the REE concentrations in the n-distributed data are of average values, whereas anomalously high REE values are only observed in the outliers. As opposed to FA carried out on n-distributed data, the most important factor (F1) on the outliers is characterized by positive weightings of elements (i.e., Zr, V, Hf, U, TiO_2) typically hosted in the detrital component of the bauxite ore. Cerium shows a negative weighting in the first factor, supporting that its deportment is controlled by the supergene remobilization process, rather than the

detrital input of primary minerals (e.g., LREE-phosphates). A clear bauxitization-related interelemental association only occurs in the F4, where lanthanides show negative weightings whereas elements indicating a typical bauxitization-related geochemical footprint (Al_2O_3, TiO_2 and Ga) are characterized by positive weightings. This might indicate that the outliers-related high REE contents are likely associated with the occurrence of detrital minerals, like monazite and xenotime, rather than being derived from the formation of authigenic minerals or enrichments due to the bauxitization process. This feature demonstrates that statistically significant REE concentrations in bauxites are not related to the presence of specific REE minerals, but at the diffuse incorporation of these elements in Al-hydroxides and Fe-oxy-hydroxides (Mondillo et al., 2019).

6.2. Nature of the bauxite parent rock

Although weathering played a great role in determining the various interelemental relationships of the bauxite deposits of SE France, when comparing these bauxites with other coeval bauxites originally located on the southern European and north African-Adria margins, it is still possible to obtain key information about the nature of the parental material. Specifically, it is possible to exclude any magmatic rock of mafic affinity as a source for bauxite of the southern European margin. In fact, bauxites directly derived from mafic parent rocks, such as those from Greece and likely Apulia, have very different compositions, characterized by high TiO_2/Al_2O_3 (~0.10) and Eu/Eu* ratios (~0.7–0.8) and very low Zr/Cr ratios (~0.5) (Mongelli et al., 2014, 2016; Mondillo et al., 2022). Instead, the bauxites of SE France are geochemically more similar to the Sardinian and the Catalan bauxites (Reinhardt et al., 2018; Mameli et al., 2020), which both show very high Zr/Cr ratios (from 1 to 49 and lower TiO_2/Al_2O_3 (~0.05) and Eu/Eu* ratios (between 0.6 and 0.7; Fig. 13). Looking in detail at this bauxite group, it is possible to notice that the southern France bauxites have a mean Eu/Eu* ratio of 0.61 (Provence) and 0.62 (Languedoc), which are lower than both the Sardinian and Catalan ones (both with a mean Eu/Eu* = 0.66; Mameli et al., 2020; Reinhardt et al., 2018) (Fig. 13). This suggests that the southern France bauxites had a slightly more felsic protore than Sardinia and Spain deposits.

The U-Pb signal recorded in the detrital zircon from France bauxites (including the recent dataset from Marchand et al., 2021) can be interpreted in the light of possible zircon reservoirs from the surrounding crystalline massifs and other potential source rocks. To this endeavor, we compiled available U-Pb data of crystalline formations from the eastern French Massif Central, including the Cévennes area (Chelle-Michou et al., 2017; Couzinié et al., 2017, 2019, 2021, 2022; Laurent et al., 2017) and the Montagne Noire (Faure et al., 2010, 2014; Poilvet et al., 2011; Pitra et al., 2012, 2022; Roger et al., 2015; Whitney et al., 2015, 2020; Lin et al., 2016; Padel et al., 2017; Trap et al., 2017; Poujol et al., 2017; Pfeifer et al., 2018) (Fig. 14A). In addition, we included U-Pb zircon data from the Languedoc Cretaceous sedimentary rocks sampled by Marchand et al. (2021), i.e., the Albian glauconitic sandstones overlying the Villeveyrac bauxite and the Valanginian marls from St Martin de Londres, and also the existing data for sedimentary rocks of Upper Cretaceous Alpine Tethys, i.e., Piedmont-Ligurian Basin, from the Western Alps (Chu et al., 2016; Mueller et al., 2018, 2020).

Compiled spectra from the eastern French Massif Central and the Montagne Noire all display a characteristic north Gondwana

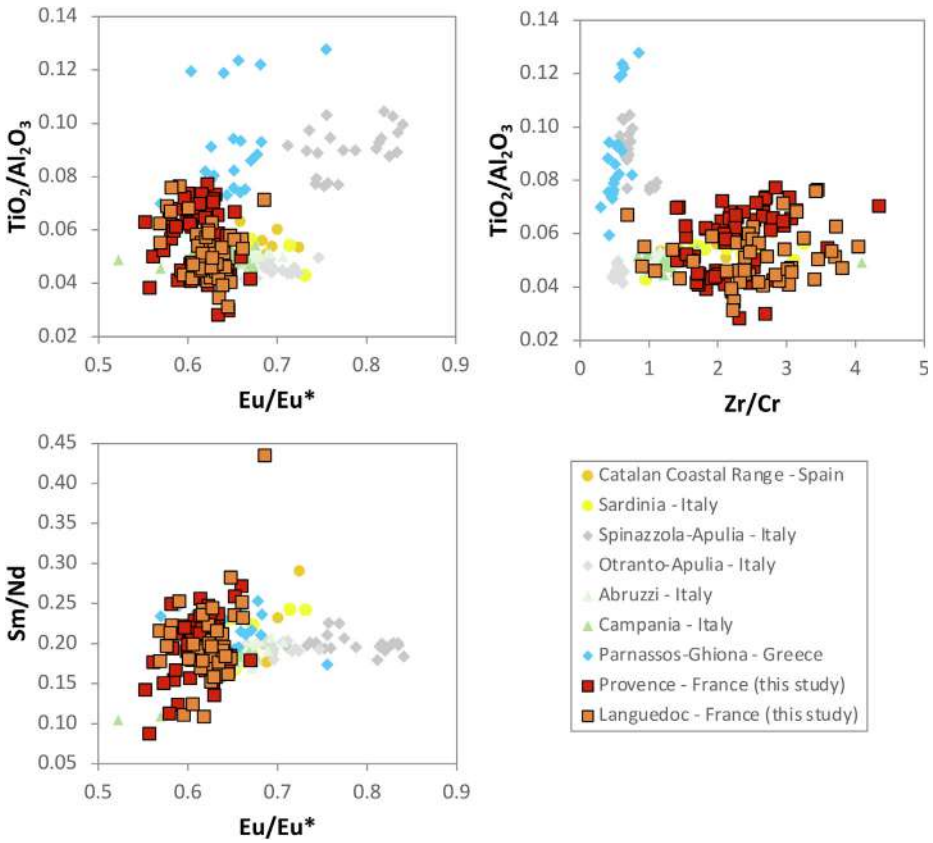

Fig. 13. Geochemical discrimination plots of (A) TiO_2/Al_2O_3 vs. Eu/Eu*, (B) TiO_2/Al_2O_3 vs. versus Zr/Cr and (C) Sm/Nd versus Eu/Eu* of bauxite samples from southern France, and the Mediterranean area. Data from: Catalan Coastal Range – Spain (Reinhardt et al., 2018); Sardinia – Italy (Mameli et al., 2020); Spinazzola-Apulia – Italy (Mongelli et al., 2014); Otranto-Apulia – Italy (Mongelli et al., 2016); Abruzzi – Italy (Putzolu et al., 2018); Campania – Italy (Boni et al., 2013); Parnassos-Ghiona – Greece (Mondillo et al., 2022).

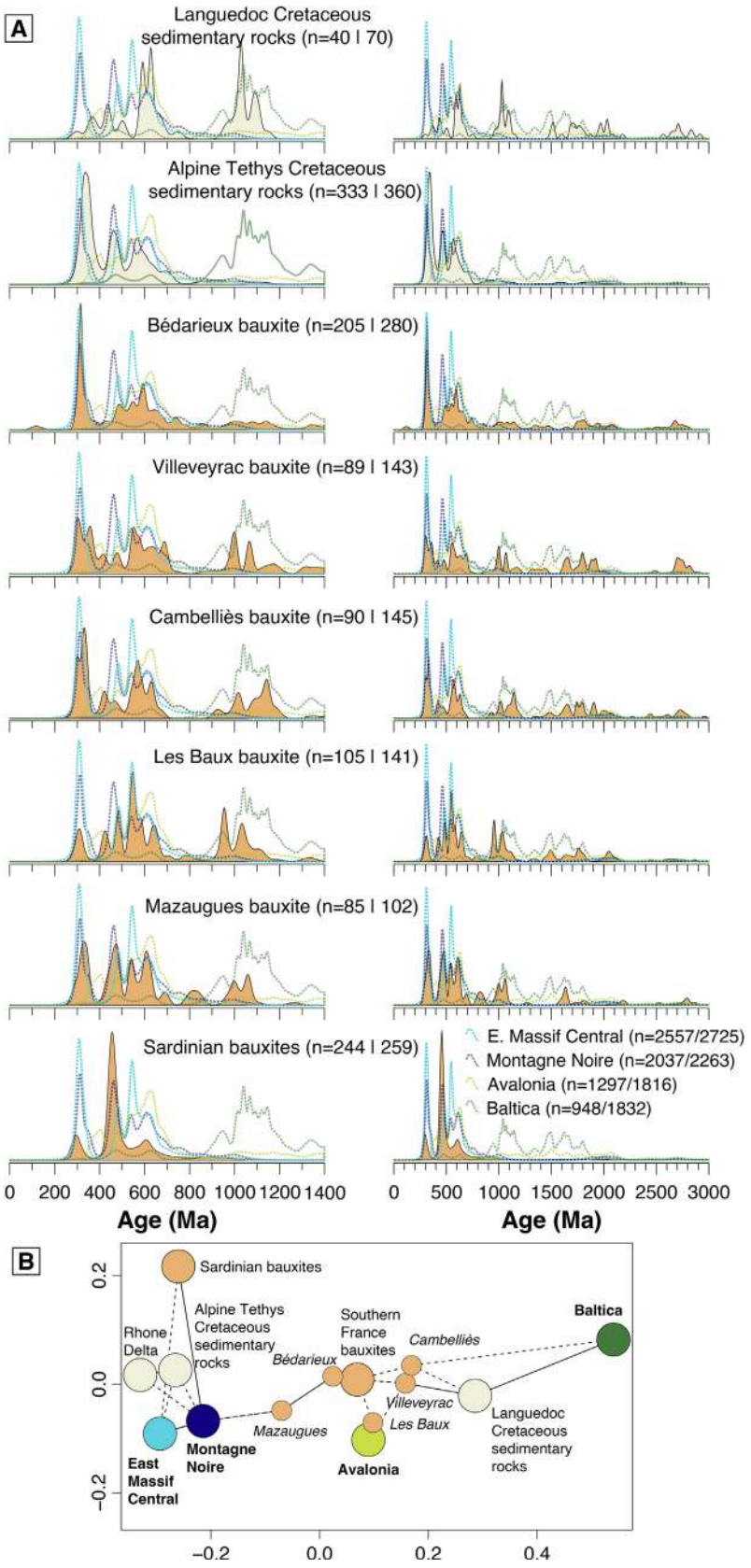

Fig. 14. A. Comparison of detrital zircon U-Pb age kernel density estimates from several southern France bauxite deposits (Les Baux and Mazaugues from this study; Bédarieux, Villeveyrac, Cambelliès from Marchand et al., 2021), from Sardinian bauxites (Yu et al., 2023), from Alpine Tethys Cretaceous sedimentary rocks from the Western and Ligurian Alps (Chu et al., 2016; Mueller et al., 2018, 2020), and from Cretaceous sedimentary rocks from Languedoc (Marchand et al., 2021). Spectra from the crystalline basements of the eastern Massif Central and the Montagne Noire are compiled from Chelle-Michou et al. (2017), Couzinié et al. (2017, 2019, 2021, 2022), Laurent et al. (2017), and from Faure et al. (2010, 2014), Pitra et al. (2012, 2022), Poilvet et al. (2011), Roger et al. (2015), Whitney et al. (2015, 2020), Lin et al. (2016), Padel et al. (2017), Trap et al. (2017), Poujol et al. (2017), Pfeifer et al. (2018), respectively. Detrital spectra from Baltica and Avalonia are from Stephan et al. (2019). The numbers in parenthesis correspond to the number of concordant U-Pb dates between 0 and 1400 Ma, vs the total number of concordant dates, respectively. B. Non-metric multidimensional scaling plot (Vermeesch, 2013) of zircon age datasets from southern France bauxites, Sardinian Bauxites (Yu et al., 2023), Alpine Tethys Cretaceous sedimentary rocks from the Western Alps and the Languedoc, modern sediments from the Rhone River delta (Avigad et al., 2022), as well as potential sources from the eastern Massif Central, the Montagne Noire, Avalonia, and Baltica.

signature (440–650 Ma, with peaks around 600, 550, and 470 Ma) overprinted by the Variscan orogeny (290–360 Ma) (Fig. 14A). They also display minor peaks at 2.7–3.3 Ga, 1.9–2.1 Ga, 0.9–1.1 Ga and a characteristic dearth of zircon record in between. Detrital zircons sampled in the Rhône delta (Avigad et al., 2022) show that modern rivers draining through the Western Alps and the eastern Massif Central mimic this pattern, further demonstrating the strong north Gondwanan affinity of this region (Chelle-Michou et al., 2017).

The detrital zircon record from the France bauxites and that of the Languedoc Lower Cretaceous sedimentary rocks somewhat contrast with this regional pattern. Indeed, from Languedoc to Provence, all bauxites are characterized by a prominent Stenian-Tonian peak (0.9–1.2 Ga) together with a relatively abundant zircon population spreading across the late Paleoproterozoic (1.6–2.1 Ga) (Fig. 14A). While all deposits feature a clear late-Variscan peak centered around 310–330 Ma, they reveal slight differences in the Silurian–Ediacaran interval. On the westernmost and easternmost sides of the studied region, Silurian to Ediacaran detrital zircon dates strongly match the record from the crystalline massifs, Montagne Noire and the eastern Massif Central, at the Bédarieux and Mazaugues deposits, respectively. In turn, while the detrital record at Les Baux, Cambelliès and Villeveyrac deposits returns comparable Ediacaran peaks (at ca. 550 and 630 Ma), each of the three deposits features unique properties. At Villeveyrac detrital zircon ages keep record of an additional Cryogenian peak (ca. 680 Ma). Both Villeveyrac and Les Baux yield an early Ordovician population (ca. 480 Ma), which is absent from Cambelliès. In turn, Cambelliès and Les Baux yield a peculiar Silurian population (peaking at ca. 430 Ma) (Fig. 14A).

It is noteworthy that Albian glauconitic sandstones from the Languedoc area lack the Cadomian (ca. 550 Ma) and late Variscan (ca. 310 Ma) peaks and rather display prominent peaks at 590–630 Ma and 950–1150 Ma, as well as Ordovician to Devonian and late Paleoproterozoic secondary populations of ages. Instead, the Alpine Tethys Upper Cretaceous sedimentary rocks of Western Alps display a north Gondwana signature (440–650 Ma) overprinted by the Variscan orogeny (290–360 Ma).

Collectively, the new data suggest that zircons in southern France have been derived from at least two contrasted sources in various proportions with no apparent regional zoning (with the currently available data). The first source yields a typical north Gondwana affinity and is most likely represented by the crystalline massifs on the Montagne Noire and the eastern Massif Central, which were likely outcropping by the Early Cretaceous (Thiry et al., 2006; Barbarand et al., 2020). In turn, the other source(s) yields age peaks unknown from Gondwana-derived terranes with affinities to Avalonian and Baltican detritus (cf. Stephan et al., 2019 for a recent compilation) and dominates also the record of the Languedoc Lower Cretaceous sedimentary rocks analyzed by Marchand et al. (2021). Available paleogeographic reconstructions of emerged continental areas during the Lower to mid-Cretaceous (Thiry et al., 2006; Barbarand et al., 2020) suggest that direct detrital routing from Avalonia or (even more) Baltica to the Vocontian and South Provence Basins would be a strained hypothesis. Instead, we propend for an alternative hypothesis, which invokes the existence of an intermediate storage of previously deposited Avalonia/Baltica detritus in a yet unknown (Variscan?) basin located in the catchment area of the Vocontian and South Provence Basins during the Lower to mid-Cretaceous. The virtual absence of these peaks in the detrital zircon record from the Alpine Tethys Cretaceous sedimentary rocks from the Western Alps, from the Sardinian Cretaceous bauxites (Yu et al., 2023), and from the modern Rhone River delta (Avigad et al., 2022), suggests that in the Lower Cretaceous, southern France experienced an episodic and local diversification in detritus provenance, with exotic material deriving from Avalonia and/or Baltica.

A multidimensional scaling analysis (Vermeesch, 2013) confirms the qualitative assessment presented above (Fig. 14B). It shows that the Alpine Tethys Cretaceous sedimentary rocks from Western Alps, the Sardinian Cretaceous bauxites, and the Rhone delta sediments, plot in close proximity to the east Massif Central and Montagne Noire basement rocks, consistent with their location and proximal source. However, this analysis also reveals that while the two crystalline massifs are very similar to each other and plot in the same region of the multidimensional space, the Languedoc Lower Cretaceous sediments consistently plot away from these, towards the detrital pattern characteristics of Avalonia and Baltica. The French bauxites plot in between the crystalline massifs and the Avalonia and Baltica detritus (Fig. 14B). This confirms that the Languedoc Lower to Mid-Cretaceous sedimentary rocks and the bauxite protore were sourced from both the outcropping Variscan massifs and an unknown Avalonia/Baltica-like source in different proportions.

Irrespective of the exact nature of this Avalonia and Baltica exotic source, it did not contribute detritus to Alpine Tethys Upper Cretaceous sediments from the Western Alps or in mid-Cretaceous bauxites of Sardinia, supporting the occurrence of a paleogeographic arrangement preventing direct sedimentary supply across southern France to the latest regions since Early Cretaceous. Unfortunately, no zircon dating is available for the Spanish bauxites or lateritic paleosoils on the Ebro block (e.g., Yuste et al., 2014; Reinhardt et al., 2018; Laita et al., 2020). This prevents any direct comparison with the presented data. However, Cretaceous sedimentary rocks from the Pyrenees display a strong Variscan peak (see the appendix of McCarthy et al., 2020), suggesting that the basement in the Iberia-Ebro block was already exposed to erosion in that period. At the same time, sedimentary rocks from the Pyrenees lack the Avalonia and Baltica component (McCarthy et al., 2020), confirming the peculiar diversification in detritus provenance characterizing the coeval Southern France sediments.

Following Barbarand et al. (2020) a significant (>1–2 km thick, depending on the area) sedimentary cover deposited in present-day sedimentary realm (Causses domain, South-East and Aquitaine basins boundaries) but also over the present-day southern border of the Massif Central during Jurassic to Early Cretaceous. Since the Aptian, the Durance stage implied the uplift of several areas, producing a widespread erosion of the preexisting sedimentary cover, which was eroded during a main episode at the end of Early Cretaceous, and in all cases before the beginning of Late Cretaceous (Barbarand et al., 2020). This erosion-dominated model is clearly contrasting with the possible development of extensive lateritic profiles above the basement during this period, because it would allow the formation of lateritic bauxites only around the Cenomanian, i.e., when several investigated bauxite deposits were already covered. The southern areas, instead, were uplifted to a lesser extent, as the level of erosion changed from an area to another (Barbarand et al., 2020). This favored chemical weathering, which resulted in the development of karst features in the Jurassic carbonates and the formation of bauxites. From the interpretation of our data, and comparison with previous work, we propose that bauxites formed at the expense of siliciclastic material derived from the mechanical erosion of uplifted proximal (Massif Central, Montagne Noire) and distal (unknown with Avalonia/Baltica affinity) basement rocks. Weathering of the mixed material could develop in-situ, in association with and/or followed by sedimentary reworking of the new-formed bauxitic soils. The degree of reworking was variable on the basis of the locality. We think that this model can explain all the characteristics of the studied bauxite deposits (e.g., Lajoinie and Laville, 1979; Combes, 1990; Chanvry et al., 2020: Marchand et al., 2021) and is in agreement with features that can be observed in environments with lateritic bauxites not very dissimilar from the mid-Cretaceous setting of southern

France (e.g., the Guyana coastal area; Monsels and van Bergen, 2017, 2019).

6.3. Implications for plate kinematics

Our research contributes to the ongoing debate regarding the kinematics of the eastern segment of the Iberia-Eurasia plate margin during the mid-Cretaceous period (Fig. 1). This long-lasting debate arises from the challenge of reconciling geological data from the Iberia-Eurasia margin, paleomagnetic data from Europe and Iberia, and magnetic anomalies observed in the Atlantic Ocean and the Bay of Biscay within a unified plate tectonic framework. A demonstrative example of the complex nature of the debate is that, despite advancements over the past five decades, each of the three margin configurations (i.e., convergent, divergent, and transform), already proposed by Choukroune et al. (1973), continues to gather substantial support. The emergence of the concept of non-rigid plates and diffuse plate boundaries (Gordon, 1998), and its application to the Iberia-Eurasia margin (e.g., Angrand and Mouthereau, 2021; Frasca et al., 2021), is likely bridging the gaps. Specifically, the identification of the Ebro block as a pivotal lithospheric feature, which during the mid-Cretaceous underwent semi-independent movements between Iberia and Eurasia (Tugend et al., 2015), marked a significant paradigm shift. This concept has increased the degrees of freedom in the mid-Cretaceous plate reconstruction of the area, increasing the weight of geological data for these reconstructions. Indeed, the recent trend is to utilize geological data from the Ebro block to trace tectonic stages and constrain geodynamics, rather than vice versa. Regional works on the Cretaceous of the area, including basin and facies analysis (e.g., Debroas, 1990; Combes, 1990), petrography (e.g., Lagabrielle et al., 2010), structural geology (e.g., Tavani et al., 2018), HT-LP metamorphism (e.g., Clerc et al., 2015; Ducoux et al., 2021), and denudation history (e.g., Curnelle and Dubois, 1986; Olivetti et al., 2020; Barbarand et al., 2020), are complemented by our data, all together providing the smoking gun of a mid-Cretaceous divergent margin, characterized by a remarkable lateral segmentation. The mid-Cretaceous bauxite deposits of the SE France basin, Iberia, and Sardinia reveal a distinctive regional arrangement, with a northern and a southern ribbon of uplifted terrains symmetrically bounding the main mid-Cretaceous deep basins within the region (Fig. 15). The formation of these mid-Cretaceous bauxites evidences a denudation stage that overlaps with the final stage of the formation of these basins. Hyperextension and mantle exhumation in the Pyrenean Rift indeed lasted from Aptian to Cenomanian (e.g., Jammes et al., 2009; Lagabrielle et al., 2010; Masini et al., 2014), whereas extension in the South Provence Basin occurred from Berriasian/Valanginian to Cenomanian (e.g., Tavani et al., 2018). Mid-Cretaceous bauxites can thus be interpreted as induced by the uplift of the basins' shoulders, which is a distinctive feature of rift systems (e.g., Buck, 1986; Weissel and Karner, 1989). Coherently, we propose that the bauxites of Sardinia and SE France developed on the two conjugate margins of the South Provence Basin, a basin floored by hyperextended continental crust (e.g., Bestani et al., 2016), which during the mid-Cretaceous was forming an eastern segment of the Bay of Biscay-Pyrenean rift system, thus supporting the geodynamic models of both Fig. 1B (e.g., Tavani et al., 2018; Balansa et al., 2022) and Fig. 1D (Angrand and Mouthereau,

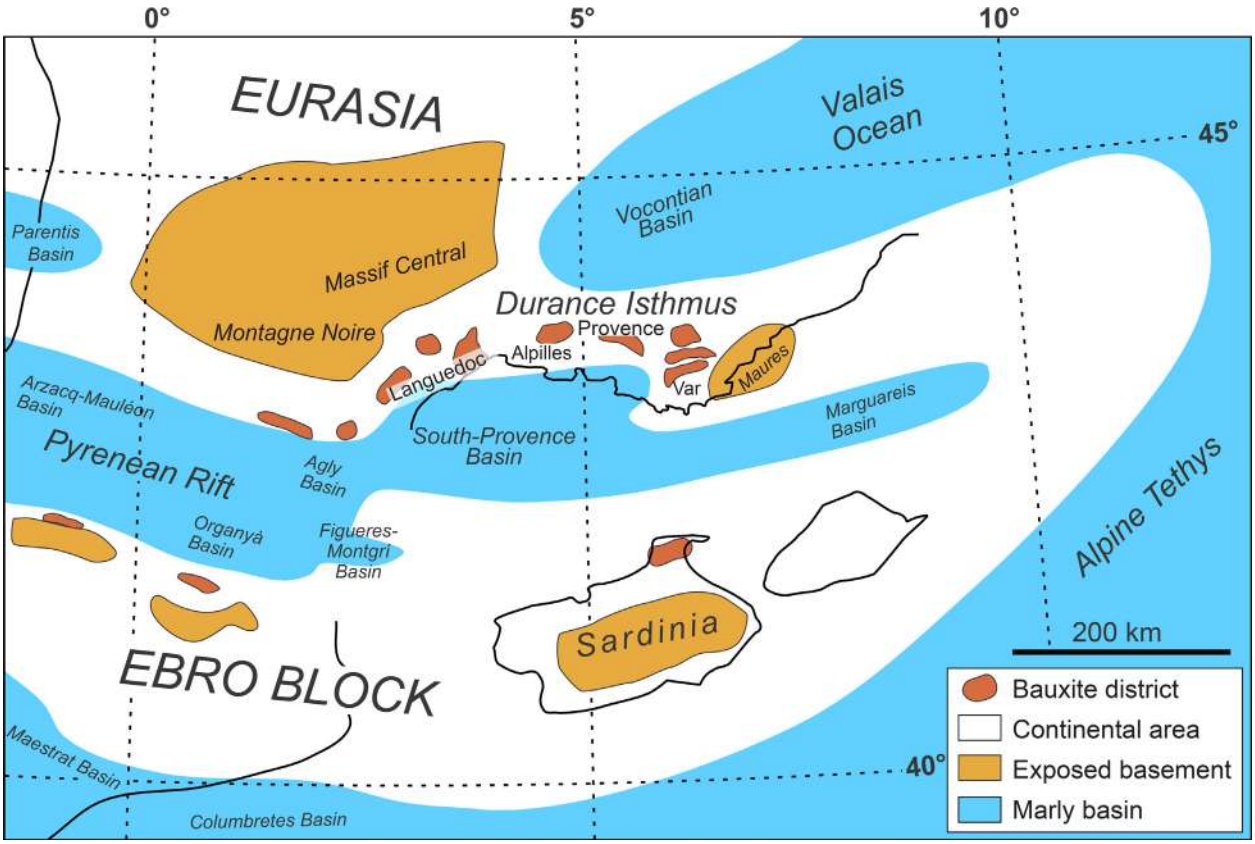

Fig. 15. Reconstruction of junction between Alpine Tethys and Pyrenean Rift and surrounding areas in the mid-Cretaceous times, with major basins, continental areas, exposed basements, and bauxite districts. Tectonic reconstruction derives from the model of Tavani et al. (2018), Angrand and Mouthereau (2021), and Balansa et al. (2022). The position of Sardinia disconnected from Durance Isthmus follows the reconstruction of Bestani et al. (2016) for the Santonian stage and has been confirmed by the present provenance study. Bauxite districts were depicted from (Combes, 1990). The positions of the exposed basements derive from Thiry et al. (2006) and Barbarand et al. (2020). Current European coastline has been indicated for reference.

2021). In summary, the strong difference we found in the bauxites of Sardinia and SE France supports those tectonic reconstructions in which Sardinia during the mid-Cretaceous was part of the Iberia-Ebro block (e.g., Handy et al., 2010; Tavani et al., 2018; Mameli et al., 2020; Balansa et al., 2022). In this context, the recognition of the Vocontian basin as the westernmost toe of the Valais Ocean (Célini et al., 2023) prevents placing any mid-Cretaceous connection between the Valais Ocean and the Pyrenean Rift and identifies the Durance Isthmus as a continental bridge connecting the tips of these two rifts (Fig. 15).

7. Conclusions

The present study revealed that the southern France karst bauxites were related to in-situ weathering processes overprinted to, or associated with, local sedimentary reworking. This genesis echoes the so-called *parallochthonous* and *parautochthonous* models of Combes (1990). The statistical analysis of geochemical data clearly indicates that the investigated bauxites have a homogenous geochemical footprint. This would be more likely due to the development of an extensive bauxitization process, which overrode any primary geochemical diversity potentially existing between the various analyzed deposits. U-Pb zircon dating on bauxite samples from the Les Baux de Provence and Mazaugues deposits sheds new light on the paleogeography at the time of bauxite formation. While the U-Pb zircon data confirm that the protores of Provence bauxites partly derived from Variscan basement rocks, the data evidence an exotic source with age peaks unknown from Gondwana-derived terranes and with affinities to Avalonian and Baltican detritus. The virtual absence of this affinity in the detrital zircon record from Alpine Tethys Cretaceous sedimentary rocks from the Western Alps and from Sardinian Cretaceous bauxites (Yu et al., 2023), suggests that in the Lower Cretaceous, southern France experienced an episodic and local diversification in detritus provenance, with exotic material deriving from Avalonia and/or Baltica or from an intermediate storage of previously deposited Avalonia/Baltica detritus in a yet unknown massif. This also supports the occurrence of a through between the European margin and Sardinia-Iberia block. The spatial arrangement of the mid-Cretaceous bauxite deposits of the SE France, Iberia, and Sardinia suggests that they formed on shoulder of uplifted terrains symmetrically bounding the main mid-Cretaceous rift-related basins within the region. Coherently, we propose that the bauxites of Sardinia and SE France developed on the two conjugate margins of the South Provence Basin.

CRediT authorship contribution statement

Nicola Mondillo: Writing – review & editing, Writing – original draft, Supervision, Project administration, Funding acquisition, Data curation, Conceptualization. **Cyril Chelle-Michou:** Writing – review & editing, Formal analysis, Data curation, Conceptualization. **Francesco Putzolu:** Writing – review & editing, Data curation. **Giuseppina Balassone:** Formal analysis. **Angela Mormone:** Formal analysis. **Licia Santoro:** Funding acquisition, Formal analysis. **Salvatore Cretella:** Formal analysis. **Gennaro Scognamiglio:** Formal analysis. **Marcella Tarallo:** Formal analysis. **Stefano Tavani:** Writing – review & editing, Supervision, Conceptualization.

Declaration of competing interest

The authors declare that they have no known competing financial interests or personal relationships that could have appeared to influence the work reported in this paper.

Acknowledgements

Our acknowledgements go to M. Séranne and E. Marchand for field guidance and discussion. We are grateful to the Associate Editor Li Tang for the editorial handling, and to M. Séranne, R. Aubrecht, and the third anonymous reviewer for fruitful comments and suggestions, which greatly enhanced the quality of the paper. The research received funding from the "Programma per il finanziamento della ricerca di Ateneo 2016–Progetto CEB", granted by Università degli Studi di Napoli Federico II (Italy) to N. Mondillo. Other funding derived from the European Union's Horizon 2020 research and innovation program, supporting the Marie Skłodowska-Curie Individual Fellowship (Project name GOSSAN, number 751103) of L. Santoro (2018).

Appendix A. Supplementary material

Supplementary data to this article can be found online at https://doi.org/10.1016/j.gr.2024.09.012.

References

Angrand, P., Mouthereau, F., 2021. Evolution of the Alpine orogenic belts in the Western Mediterranean region as resolved by the kinematics of the Europe-Africa diffuse plate boundary. B. Soc. Geol. Fr. 192 (1), 42. https://doi.org/10.1051/bsgf/2021031.

Arnaud, H., Ferry, S., Masse, J. P., 1984. Crétacé Inférieur, Planche Ci7. In S. Debrand-Passard, and S. Courbouleix (Eds.), Synthèse Géologique Du Sud-Est De La France. Mem. 126. Orléans, France: BRGM.

Avigad, D., Abbo, A., Gerdes, A., Schmitt, A.K., 2022. Crustal evolution of Western Europe: constraints from detrital zircon U-Pb-Hf-O isotopes. Gondw. Res. 106, 379–396. https://doi.org/10.1016/j.gr.2022.02.006.

Bache, F., Olivet, J.L., Gorini, C., Aslanian, D., Labails, C., Rabineau, M., 2010. Evolution of rifted continental margins: the case of the Gulf of Lions (Western Mediterranean Basin). Earth Planet. Sci. Lett. 292 (3–4), 345–356. https://doi.org/10.1016/j.epsl.2010.02.001.

Balansa, J., Espurt, N., Hippolyte, J.-C., Philip, J., Caritg, S., 2022. Structural evolution of the superimposed Provençal and Subalpine fold-thrust belts (SE France). Earth Sci. Rev. 227, 103972. https://doi.org/10.1016/j.earscirev.2022.103972.

Barbarand, J., Lucazeau, F., Pagel, M., Séranne, M., 2001. Burial exhumation history of the southern–eastern Massif Central (France) constrained by apatite fission-track thermochronology. Tectonophysics 335, 275–290. https://doi.org/10.1016/S0040-1951(01)00069-5.

Barbarand, J., Préhaud, P., Baudin, F., Missenard, Y., Matray, J.M., François, T., Blaise, T., Pinna-Jamme, R., Gautheron, C., 2020. Where are the limits of Mesozoic intracontinental sedimentary basins of southern France? Mar. Petrol. Geol. 121, 104589. https://doi.org/10.1016/j.marpetgeo.2020.104589.

Bárdossy, G., 1982. Karst Bauxites. Developments in Economic Geology vol. 14, 441 p.

Bárdossy, G., Aleva, J.J., 1990. Lateritic Bauxites. Elsevier, Amsterdam, p. 624 p.

Beaudrimont, A. F., Dubois, P., 1977. Un Bassin Mésogéen Du Domaine Péri-Alpin: Le Sud-Est De La France. B. Centres Rech. Explor.-Prod. Elf Aquitaine, 1, 261–308.

Bergerat, F., 1987. Stress fields in the European platform at the time of Africa-Eurasia collision. Tectonics 6, 99–132.

Bertier, P., 1821. Analyse de l'alumine hydrateé des Beaux, department des Bouches-du-Rhone. Ann. Min. Paris, 1st series, 6, 531–534.

Bestani, L., Espurt, N., Lamarche, J., Bellier, O., Hollender, F., 2016. Reconstruction of the Provence Chain evolution, southeastern France. Tectonics 35 (6), 1506–1525. https://doi.org/10.1002/2016TC004115.

Boni, M., Rollinson, G., Mondillo, N., Balassone, G., Santoro, L., 2013. Quantitative mineralogical characterization of karst bauxite deposits in the Southern Apennines. Italy. Econ. Geol. 108, 813–833. https://doi.org/10.2113/econgeo.108.4.813.

Bonijoly, D., Perrin, J., Roure, F., Bergerat, F., Courel, L., Elmi, S., GPF team, Mignot, A. 1996. The Ardèche paleomeargin of the South-East Basin of France: Mesozoic evolution of a part of the Tethyan continental margin. Mar. Petrol. Geol. 13, 607–623. doi: 10.1016/0264-8172(95)00075-5.

Bourquin, S., Bercovici, A., Lopez-Gimez, J., Diez, J.B., Broutin, J., Ronchi, A., Durand, M., Arché, A., Linol, B., Amour, F., 2011. The Permian-Triassic transition and the onset of Mesozoic sedimentation at the northwestern peri-Tethyan domain scale: Palaeogeographic maps and geodynamic implications. Palaeogeogr. Palaeocl. Palaeoecol. 299, 265–280. https://doi.org/10.1016/j.palaeo.2010.11.007.

BRGM, 2005. Cartes géologiques vectorisées et harmonisées à 1/50 000 du BRGM, https://infoterre.brgm.fr/formulaire/telechargement-cartes-geologiques-departementales-150-000-bd-charm-50.

Bruguier, O., Becq-Giraudon, J.F., Bosch, D., Lancelot, J.R., 1998. Late Visean hidden basins in the internal zones of the Variscan belt: U-Pb zircon evidence from the French Massif Central. Geology 26, (627–630).
Bruguier, O., Becq-Giraudon, J.F., Champenois, M., Deloule, E., Ludden, J., Mangin, D., 2003. Application of in situ zircon geochronology and accessory phase chemistry to constraining basin development during post-collisional extension: A case study from the French Massif Central. Chem. Geol. 201, 319–336. https://doi.org/10.1016/j.chemgeo.2003.08.005.
Buck, W.R., 1986. Small-scale convection induced by passive rifting: the cause for uplift of rift shoulders. Earth Planet. Sc. Lett. 77 (3–4), 362–372.
Célini, N., Mouthereau, F., Lahfid, A., Gout, C., Callot, J.P., 2023. Rift thermal inheritance in the SW Alps (France): insights from RSCM thermometry and 1D thermal numerical modelling. Solid Earth 14 (1), 1–16. https://doi.org/10.5194/se-14-1-2023.
Champion, C., Choukroune, P., Clauzon, G., 2000. La déformation post-Miocène en Provence occidentale. Geodin. Acta 13, 67–85.
Chanvry, E., Marchand, E., Lopez, M., Séranne, M., Le-Sout, G., Vinches, M., 2020. Tectonic and climate control on allochthonous bauxite deposition. Example from the mid-Cretaceous Villeveyrac basin, Southern France. Sed. Geol. 407, 105727. https://doi.org/10.1016/j.sedgeo.2020.105727.
Chelle-Michou, C., Laurent, O., Moyen, J.-F., Block, S., Paquette, J.-L., Couzinié, S., Gardien, V., Vanderhaeghe, O., Villaros, A., Zeh, A., 2017. Pre-Cadomian to late-Variscan odyssey of the eastern Massif Central, France: Formation of the West European crust in a nutshell. Gondw. Res. 46, 170–190. https://doi.org/10.1016/j.gr.2017.02.010.
Choukroune, P., Le Pichon, X., Seguret, M., Sibuet, J.C., 1973. Bay of Biscay and Pyrenees. Earth Planet. Sci. Lett. 18, 109–118.
Chu, Y., Lin, W., Faure, M., Wang, Q., 2016. Detrital zircon U-Pb ages and Hf isotopic constraints on the terrigenous sediments of the Western Alps and their paleogeographic implications. Tectonics 35, 2734–2753. https://doi.org/10.1002/2016tc004276.
Clerc, C., Lahfid, A., Monié, P., Lagabrielle, Y., Chopin, C., Poujol, M., Boulvais, P., Ringenbach, J.-C., Masini, E., de St Blanquat, M., 2015. High-temperature metamorphism during extreme thinning of the continental crust: a reappraisal of the North Pyrenean passive paleomargin. Solid Earth 6 (2), 643–668. https://doi.org/10.5194/se-6-643-2015.
Combes, P.J., 1972. Les différents types de bauxites sur substratum carbonate dans le Languedoc et l'Ariège. Remarques sur la notion d'allochtonie et d'autochtonie. C.R. Acad. Sc. Paris 274, 1613–1616.
Combes, P.J., 1973. Etude géologique sur les conditions de mise en place d'une bauxite allochtone a substratum carbonate: le gisement de Bédarieux (Hérault, France). I.C.S.O.B.A., 2nd Congr. Int. Nice 1973, 89–108.
Combes, P.J., 1984. Regards sur la géologie des bauxites; aspects récents sur la genèse de quelques gisements a substratum carbonate. B. Centres Rech. Explor. Prod. Elf Aquitaine 8, 251–274.
Combes, P.J., 1990. Typologie, Cadre Géodynamique Et Genèse Des Bauxites Françaises. Geodin. Acta 2, 91–109.
Combes, P.J., 1969. Recherches Sur La Genèse Des Bauxites Dans Le Nord-Est De L'espagne, La Languedoc Et L'arige (France) Montpellier. Mém. CERH, III-IV, 1–342.
Coquand, H., 1871. Sur les bauxites de la chaine des Alpines (Bouches-du-Rhone) et leur age géologique. B. Soc. Geol. Fr. 28, 98–115.
Costamagna, L.G., 2023. Sardinia and the Alpine cycle: A tectono-sedimentary history at the Western Tethys edge. Earth Sci. Rev. 247, 104591. https://doi.org/10.1016/j.earscirev.2023.104591.
Cotillon, P., 1984. Crétacé Inférieur. In S. Debrand-Passard, & S. Courbouleix (Eds.), Synthèse Géologique Du Sud-Est De La France, BRGM Mem. 126, 287–387.
Couzinié, S., Laurent, O., Poujol, M., Mintrone, M., Chelle-Michou, C., Moyen, J.-F., Bouilhol, P., Vezinet, A., Marko, L., 2017. Cadomian S-type granites as basement rocks of the Variscan belt (Massif Central, France): Implications for the crustal evolution of the north Gondwana margin. Lithos 286–287, 16–34. https://doi.org/10.1016/j.lithos.2017.06.001.
Couzinié, S., Laurent, O., Chelle-Michou, C., Bouilhol, P., Paquette, J.-L., Gannoun, A.-M., Moyen, J.-F., 2019. Detrital zircon U-Pb–Hf systematics of Ediacaran metasediments from the French Massif Central: Consequences for the crustal evolution of the north Gondwana margin. Precambr. Res. 324, 269–284. https://doi.org/10.1016/j.precamres.2019.01.016.
Couzinié, S., Bouilhol, P., Laurent, O., Marko, L., Moyen, J.-F., 2021. When zircon drowns: Elusive geochronological record of water-fluxed orthogneiss melting in the Velay dome (Massif Central, France). Lithos 384, 105938. https://doi.org/10.1016/j.lithos.2020.105938.
Couzinié, S., Bouilhol, P., Laurent, O., Grocolas, T., Montel, J.-M., 2022. Cambro-Ordovician ferrosilicic magmatism along the northern Gondwana margin: constraints from the Cézarenque-Joyeuse gneiss complex (French Massif Central). B. Soc. Geol. Fr. 193, 15. https://doi.org/10.1051/bsgf/2022010.
Curnelle, R., Dubois, P., 1986. Evolution mésozoique des grands bassins sédimentaires Français; bassins de Paris, d'Aquitaine et du Sud-Est. B. Soc. Geol. Fr. 2, 529–546.
D'Aoust, V., 1865. Notes minéralogiques et géologiques sur le mineral de fer alumineux pisoltique de Mouries, dit aussi de Baux, canton de Saint-Rèmy, département des Bouches-du-Rhone. B. Soc. Geol. Fr. 22, 418–420.
Dangić, A., 1985. Kaolinization of bauxite: a study in the Vlasenica bauxite area, Yugoslavia. I. Alteration of Matrix. Clay Clay Miner. 33, 517–524.
Dangić, A., 1988. Kaolinization of bauxite: a study of the Vlasenica bauxite area, Yugoslavia. II. Alteration of Oolites. Clay Clay Miner. 36, 439–447.
Daubrée, M., 1869. Note sur l'existence de gisements de bauxite dans les départements de l'Herault et de l'Ariège. B. Soc. Geol. Fr. 26, 915–918.
Debroas, E.J., 1990. Le flysch noir albo-cénomanien témoin de la structuration albienne à sénonienne de la zone nord-Pyrénéenne en Bigorre (Hautes Pyrénées, France). B. Soc. Geol. Fr. 6, 273–286.
Delfaud, J., Toutin-Morin, N., Morin, R., 1989. Un cone alluvial en bordure d'un bassin intramontagneux: La formation permienne du Rocher de Roquebrune (Bassin du Bas-Argens, Provence orientale), C. R. Acad. Sci., Ser. II: Mec., Phys., Chim. Sci. Terre Univers 309, 1811–1817.
Dieulafait, M., 1881. Les bauxites, leurs ages, leur origine. Diffusion complete du titane et du vanadium dans les roches de la formation primordiale. C. r. Acad. Sci. Paris 93, 804–807.
Ducoux, M., Jolivet, L., Cagnard, F., Baudin, T., 2021. Basement-cover decoupling during the inversion of a hyperextended basin: Insights from the Eastern Pyrenees e2020TC006512 Tectonics 40 (5). https://doi.org/10.1029/2020TC006512.
Espurt, N., Hippolyte, J.-C., Saillard, M., Bellier, O., 2012. Geometry and kinematic evolution of a long-living foreland structure inferred from field data and cross section balancing, the Sainte-Victoire system, Provence, France. Tectonics 31, 4, TC4021. https://doi.org/10.1029/2011TC002988.
Faure, M., Lardeaux, J.-M., Ledru, P., 2009. A Review of the pre-Permian geology of the Variscan French Massif Central. C.R. Geosci. 341, 202–213. https://doi.org/10.1016/j.crte.2008.12.001.
Faure, M., Cocherie, A., Mézème, E.B., Charles, N., Rossi, P., 2010. Middle Carboniferous crustal melting in the Variscan Belt: New insights from U-Th–Pbtot. monazite and U–Pb zircon ages of the Montagne Noire Axial Zone (southern French Massif Central). Gondw. Res. 18, 653–673. https://doi.org/10.1016/j.gr.2010.02.005.
Faure, M., Cocherie, A., Gach, J., Esnault, C., Guerrot, C., Rossi, P., Wei, L., Qiuli, L., 2014. Middle Carboniferous intracontinental subduction in the Outer Zone of the Variscan Belt (Montagne Noire Axial Zone, French Massif Central): multimethod geochronological approach of polyphase metamorphism. Geol. Soc. Sp. 405, 289–311. https://doi.org/10.1144/sp405.2.
Frasca, G., Manatschal, G., Cadenas, P., Miró, J., Lescoutre, R., 2021. A kinematic reconstruction of Iberia using intracontinental strike-slip corridors. Terra Nova 33 (6), 573–581. https://doi.org/10.1111/ter.12549.
Freyssinet, P., Butt, C.R.M., Morris, R.C., Piantone, P., 2005. Ore-forming processes related to lateritic weathering. Econ. Geol. 100th Ann. Vol, 681–722.
Gattacceca, J., Deino, A., Rizzo, R., Jones, D.S., Henry, B., Beaudoin, B., Vadeboin, F., 2007. Miocene rotation of Sardinia: New paleomagnetic and geochronological constraints and geodynamic implications. Earth Planet. Sc. Lett. 258, 359–377. https://doi.org/10.1016/j.epsl.2007.02.003.
Gordon, R., 1998. The plate tectonic approximation: Plate nonrigidity, diffuse plate boundaries, and global plate reconstructions. Annu. Rev. Earth Planet. Sci. 26, 615–642. https://doi.org/10.1146/annurev.earth.26.1.615.
Guendon, J.L., Parron, C., 1985. Les phenomenes karstiques dans les processus de la bauxitisation sur substrat carbonate. Exemples de gisements du sud-est de la France. Ann. Soc Géol. Belg. 108, 85–92.
Guillong, M., von Quadt, A., Sakata, S., Peytcheva, I., Bachmann, O., 2014. LA-ICP-MS Pb–U dating of young zircons from the Kos-Nisyros volcanic centre, SE Aegean arc. J. Anal. At. Spectrom 29, 963–970.
Guyonnet-Benaize, C., Lamarche, J., Masse, J.-P., Villeneuve, M., Viseur, S., 2010. 3-D structural modelling of small-deformations in poly-phase faults pattern. Application to the mid-Cretaceous Durance uplift, Provence (SE France). J. Geodyn. 50 (2), 81–93.
Guyonnet-Benaize, C., Lamarche, J., Hollender, F., Viseur, S., Münch, P., Borgomano, J., 2015. Three-dimensional structural modeling of an active fault zone based on complex outcrop and subsurface data: The Middle Durance Fault Zone inherited from polyphase Meso-Cenozoic tectonics (southeastern France). Tectonics 34, 265–289. https://doi.org/10.1002/2014TC003749.
Handy, M.R., Schmid, S.M., Bousquet, R., Kissling, E., Bernoulli, D., 2010. Reconciling plate-tectonic reconstructions of Alpine Tethys with the geological–geophysical record of spreading and subduction in the Alps. Earth Sci. Rev. 102, 121–158. https://doi.org/10.1016/j.earscirev.2010.06.002.
Hemelsdaël, R., Séranne, M., Husson, E., Ballas, G., 2021. Structural style of the Languedoc Pyrenean thrust belt in relation with the inherited Mesozoic structures and with the rifting of the Gulf of Lion margin, southern France. B. Soc. Geol. Fr. - Earth Sci. 192, 46. https://doi.org/10.1051/bsgf/2021037.
Herrington, R., Mondillo, N., Boni, M., Thorne, R., Tavlan, M., 2016. Bauxite and Nickel-Cobalt Lateritic Deposits of the Tethyan Belt. In: Richards, J., (Ed.), Tectonics and Metallogeny of the Tethyan Orogenic Belt, Special Publication, SEG Inc. Littleton, CO, USA, 2016; Vol. 19, 349–387.
Hippolyte, J.-C., Angelier, J., Bergerat, F., Nury, D., Guieu, G., 1993. Tectonic-stratigraphic record of paleostress time changes in the Oligocene basins of the Provence, southern France. Tectonophysics 226, 15–35.
Horstwood, M.S.A., Košler, J., Gehrels, G., Jackson, S.E., McLean, N.M., Paton, C., Pearson, N.J., Sircombe, K., Sylvester, P., Vermeesch, P., Bowring, J.F., Condon, D. J., Schoene, B., 2016. Community-derived standards for LA- ICP - MS U-(Th-)Pb geochronology – uncertainty propagation, age interpretation and data reporting. Geostand. Geoanal. Res. 40, 311–332.
Jammes, S., Manatschal, G., Lavier, L., Masini, E., 2009. Tectonosedimentary evolution related to extreme crustal thinning ahead of a propagating ocean: example of the western Pyrenees. Tectonics 28, TC4012. https://doi.org/10.1029/2008TC002406.

Jolivet, L., Gorini, C., Smit, J., Leroy, S., 2015. Continental breakup and the dynamics of rifting in back-arc basins: the Gulf of Lion margin. Tectonics 34 (4), 662–679. https://doi.org/10.1002/2014TC003570.
Kalaitzidis, S., Siavalas, G., Skarpelis, N., Araujo, C.V., Christanis, K., 2010. Late Cretaceous coal overlying karstic bauxite deposits in the Parnassus-Ghiona Unit, Central Greece: coal characteristics and depositional environment. Int. J. Coal Geol. 81, 211–226. https://doi.org/10.1016/j.coal.2009.06.005.
Koicki, S., Koicki, A., Maksimović, Z., 1980. Neutron activation analysis of lanthanides in Yugoslav bauxites. Glas - Srpska Akademija Nauka i Umetnosti, Odeljenje Prirodno-Matematickih Nauka, 46, 37–48.
Lacombe, O., Jolivet, L., 2005. Structural and kinematic relationships between Corsica and the Pyrenees-Provence domain at the time of the Pyrenean orogeny. Tectonics 24, TC1003. https://doi.org/10.1029/2004TC001673.
Lagabrielle, Y., Labaume, P., de Saint Blanquat, M., 2010. Mantle exhumation, crustal denudation, and gravity tectonics during Cretaceous rifting in the Pyrenean realm (SW Europe): insights from the geological setting of the lherzolite bodies. Tectonics 29 (4), TC4012. https://doi.org/10.1029/2009TC002588.
Laita, E., Bauluz, B., Aurell, M., Bádenas, B., Canudo, J.I., Yuste, A., 2020. A change from warm/humid to cold/dry climate conditions recorded in lower Barremian clay-dominated continental successions from the SE Iberian Chain (NE Spain). Sed. Geol. 403, 105673. https://doi.org/10.1016/j.sedgeo.2020.105673.
Lajoinie, J.P., Laville, P., 1980. Bauxites du Sud de la France, Synthèse Finale, Récapitulation des travaux coordonnés de 1976 à 1980. Inventaire du territoire métropolitain, Bur. Res. Geol. Min., Orléans, France, 11 p.
Lajoinie, J.P., Laville, P., 1979. Les formations bauxitiques de Provence et du Languedoc. Dimensions et distribution des gisements. Mém. Bur. Res. Geol. Min. 100, 142 p.
Laskou, M., Andreou, G., 2003. Rare earth element distribution and REE-minerals from the Parnassos-Ghiona bauxite deposits, Greece. In: Eliopoulos D. et al. (Eds.), "Mineral Exploration and Sustainable Development", 7th Biennial SGA Meeting, Athens, Millpress, Rotterdam, 89–92.
Laurent, O., Couzinié, S., Zeh, A., Vanderhaeghe, O., Moyen, J.-F., Villaros, A., Gardien, V., Chelle-Michou, C., 2017. Protracted, coeval crust and mantle melting during Variscan late-orogenic evolution: U-Pb dating in the eastern French Massif Central. Int. J. Earth Sci. 106, 421–451. https://doi.org/10.1007/s00531-016-1434-9.
Laville, P., 1981. La formation bauxitique Provençale (France). Séquence des faciès chimiques et paléomorphologie Crétacée. Chron. Rech. Min. 461, 51–68.
Li, S., Santosh, M., Indu, G., Shaji, E., Tsunogae, T., 2017. Detrital zircon geochronology of quartzites from the southern Madurai Block, India: implications for Gondwana reconstruction. Geosci. Front. 8 (4), 851–867. https://doi.org/10.1016/j.gsf.2016.07.002.
Liao, X., Wang, Y., Liu, L., Wang, C., Santosh, M., 2017. Detrital zircon U-Pb and Hf isotopic data from the Liuling Group in the South Qinling belt: provenance and tectonic implications. J. Asian Earth Sci. 134, 244–261. https://doi.org/10.1016/j.jseaes.2016.11.020.
Lin, W., Faure, M., Li, X., Chu, Y., Ji, W., Xue, Z., 2016. Detrital zircon age distribution from Devonian and Carboniferous sandstone in the Southern Variscan Fold-and-Thrust belt (Montagne Noire, French Massif Central), and their bearings on the Variscan belt evolution. Tectonophysics 677, 1–33. https://doi.org/10.1016/j.tecto.2016.03.032.
Lucas, Y., 1989. Systèmes pédologiques en Amazonie brésilienne: Equilibres, Déséquilibres et Transformations. Unpublished Ph.D. thesis, France, University of Poitiers, 153 p.
MacLean, W.H., Bonavia, F.F., Sanna, G., 1997. Argillite debris converted to bauxite during karst weathering: evidence from immobile element geochemistry at the Olmedo Deposit. Sardinia. Miner. Deposita 32, 607–616.
Maksimović, Z., Pantó, G., 1996. Authigenic rare earth minerals in karst bauxites and karstic nickel deposits. In: Jones, A.P., Wall, F. and Williams, C.T., (Eds.), Rare earth minerals, chemistry, origin and ore deposits, Chapter 10, 257–279.
Maksimović, Z., Roaldset, E., 1976. Lanthanide elements in some Mediterranean karstic bauxite deposits. Travaux ICSOBA, (International Committee for Study of Bauxite, Alumina & Aluminium). Zagreb, Croatia 13, 199–220.
Maksimović, Z., Skarpelis, N., Pantó, G., 1993. Mineralogy and geochemistry of the rare earth elements in the karstic nickel deposit of Lokris area, Greece. Acta Geol. Hungarica 36 (3), 331–342.
Mameli, P., Mongelli, G., Oggiano, G., Dinelli, E., 2007. Geological, geochemical and mineralogical features of some bauxite deposits from Nurra (Western Sardinia, Italy): insights on conditions of formation and parental affinity. Int. J. Earth Sci. 96, 887–902.
Mameli, P., Mongelli, G., Sinisi, R., Oggiano, G., 2020. Weathering Products of a Dismantled Variscan Basement. Minero-Chemical Proxies to Insight on Cretaceous Palaeogeography and Late Neogene Palaeoclimate of Sardinia (Italy). Front. Earth Sci. 8, 290. https://doi.org/10.3389/feart.2020.00290.
Marchand, E., Séranne, M., Bruguier, O., Vinches, M., 2021. LA-ICP-MS dating of detrital zircon grains from the Cretaceous allochthonous bauxites of Languedoc (south of France): Provenance and geodynamic consequences. Basin Res. 33, 270–290. https://doi.org/10.1111/bre.12465.
Marchand, E., 2019. Rôle des interactions tectonique-sédimentation sur l'évolution et la variabilité spatiale d'un gisement de bauxite karstique: exemple du bassin de Villeveyrac (Sud de France). Ph.D. thesis, Université de Montpellier-IMT Mines Alès, 374 p.
Martín-Fernández, J.A., Barceló-Vidal, C., Pawlowsky-Glahn, V., 2003. Dealing with zeros and missing values in compositional data sets using nonparametric imputation. Math. Geol. 35, 253–278.
Mascle, A., Vially, R., Deville, E., Biju-Duval, B., Roy, J.P., 1996. The petroleum evaluation of a tectonically complex area: The western margin of the Southeast Basin (France). Mar. Petrol. Geol. 13, 941–961.
Masini, E., Manatschal, G., Tugend, J., Mohn, G., Flament, J.-M., 2014. The tectonosedimentary evolution of a hyper-extended rift basin: the example of the Arzacq-Mauléon rift system (Western Pyrenees, SW France). Int. J. Earth Sci. 103 (6), 1569–1596. https://doi.org/10.1007/s00531-014-1023-8.
Masse, J.-P., Philip, J., 1976. Paléogéographie et tectonique du Crétacé moyen en Provence: Révision du concept d'isthme durancien. Rev. Geogr. Phys. Geol. Dyn. 18 (1), 49–66.
McCarthy, A., Tugend, J., Mohn, G., Candioti, L., Chelle-Michou, C., Arculus, R., Schmalholz, S.M., Müntener, O., 2020. A case of Ampferer-type subduction and consequences for the Alps and the Pyrenees. Am. J. Sci. 320 (4), 313–372. https://doi.org/10.2475/04.2020.01.
Mondillo, N., Balassone, G., Boni, M., Rollinson, G., 2011. Karst bauxites in the Campania Apennines (southern Italy): a new approach. Period. Mineral. 80, 407–432.
Mondillo, N., Balassone, G., Boni, M., Chelle-Michou, C., Cretella, S., Mormone, A., Putzolu, F., Santoro, L., Scogniamiglio, G., Tarallo, M., 2019. Rare Earth Elements (REE) in Al- and Fe-(Oxy)-Hydroxides in Bauxites of Provence and Languedoc (Southern France): implications for the potential recovery of REEs as by-products. Minerals 9. https://doi.org/10.3390/min9090504.
Mondillo, N., Di Nuzzo, M., Kalaitzidis, S., Boni, M., Santoro, L., 2022. Petrographic and geochemical features of the B3 bauxite horizon (Cenomanian-Turonian) in the Parnassos-Ghiona area: a contribution towards the genesis of the Greek karst bauxites. Ore Geol. Rev. 143, 104759. https://doi.org/10.1016/j.oregeorev.2022.104759.
Mongelli, G., 1997. Ce-anomalies in the textural components of Upper Cretaceous karst bauxites from the Apulian Carbonate Platform (southern Italy). Chem. Geol. 140, 69–79.
Mongelli, G., Acquafredda, P., 1999. Ferruginous concretions in a Late Cretaceous karst bauxite: composition and conditions of formation. Chem. Geol. 158, 315–320.
Mongelli, G., Boni, M., Buccione, R., Sinisi, R., 2014. Geochemistry of the Apulian karst bauxites (southern Italy): Chemical fractionation and parental affinities. Ore Geol. Rev. 63, 9–21. https://doi.org/10.1016/j.oregeorev.2014.04.012.
Mongelli, G., Buccione, R., Gueguen, E., Langone, A., Sinisi, R., 2016. Geochemistry of the Apulian allochthonous karst bauxite, Southern Italy: distribution of critical elements and constraints on Late Cretaceous Peri-Tethyan palaeogeography. Ore Geol. Rev. 77, 246–259. https://doi.org/10.1016/j.oregeorev.2016.03.002.
Monsels, D.A., van Bergen, M.J., 2017. Bauxite formation on Proterozoic bedrock of Suriname. J. Geochem. Explor. 180, 71–90. https://doi.org/10.1016/j.gexplo.2017.06.011.
Monsels, D.A., van Bergen, M.J., 2019. Bauxite formation on Tertiary sediments in the coastal plain of Suriname. J. S. Am. Earth Sci. 89, 275–298. https://doi.org/10.1016/j.jsames.2018.10.010.
Mueller, P., Langone, A., Patacci, M., Giulio, A.D., 2018. Detrital signatures of impending collision: the deep-water record of the Upper Cretaceous Bordighera Sandstone and its basal complex (Ligurian Alps, Italy). Sed. Geol. 377, 147–161. https://doi.org/10.1016/j.sedgeo.2018.10.002.
Mueller, P., Langone, A., Patacci, M., Giulio, A.D., 2020. Towards a Southern European Tethyan Palaeomargin provenance signature: sandstone detrital modes and detrital zircon U-Pb age distribution of the Upper Cretaceous-Paleocene Monte Bignone Sandstones (Ligurian Alps, NW Italy). Int. J. Earth Sci. 109, 201–220. https://doi.org/10.1007/s00531-019-01797-5.
Nicolas, J., 1968. Nouvelles données sur la genése des bauxites à mur karstique du sud-est de la France. Mineral. Deposita 3, 18–33.
Norton, S.A., 1973. Laterite and bauxite formation. Econ. Geol. 68, 353–361.
Nyobe, J.B., 1991. Application of normative calculations in quantitative comparative mineralogical studies of bauxite. Ore Geol. Rev. 6, 45–50.
Olivetti, V., Balestrieri, M.L., Godard, V., Bellier, O., Gautheron, C., Valla, P.G., Zattin, M., Faccenna, C., Pinna-Jamme, R., Manchuel, K., 2020. Cretaceous and late Cenozoic uplift of a Variscan Massif: the case of the French Massif Central studied through low-temperature thermochronometry. Lithosphere 12, 133–149. https://doi.org/10.1130/L1142.1.
Padel, M., Álvaro, J.J., Clausen, S., Guillot, F., Poujol, M., Chichorro, M., Monceret, E., Pereira, M.F., Vizcaïno, D., 2017. U-Pb laser ablation ICP-MS zircon dating across the Ediacaran-Cambrian transition of the Montagne Noire, southern France. C. R. Geosci. 349, 380–390. https://doi.org/10.1016/j.crte.2016.11.002.
Paton, C., Woodhead, J.D., Hellstrom, J.C., Hergt, J.M., Greig, A., Maas, R., 2010. Improved laser ablation U-Pb zircon geochronology through robust downhole fractionation correction: improved laser ablation U-Pb geochronology. Geochem. Geophys. Geosyst. 11, Q0AA06.
Paton, C., Hellstrom, J., Paul, B., Woodhead, J., Hergt, J., 2011. Iolite: Freeware for the visualization and processing of mass spectrometric data. J. Anal. At. Spectrom 26, 2508.
Petrus, J.A., Kamber, B.S., 2012. VizualAge: a novel approach to laser ablation ICP-MS U-Pb geochronology data reduction. Geostand. Geoanal. Res. 36, 247–270.
Peyaud, J.B., Barbarand, J., Carter, A., Pagel, M., 2005. Mid-Cretaceous uplift and erosion on the northern margin of the Ligurian Tethys deduced from thermal history reconstruction. Int. J. Earth Sci. 94, 462–474.
Pfeifer, L.S., Soreghan, G.S., Pochat, S., Driessche, J.V.D., Thomson, S.N., 2018. Permian exhumation of the Montagne Noire core complex recorded in the Graissessac-Lodève Basin, France. Basin Res. 30, 1–14. https://doi.org/10.1111/bre.12197.
Philip, H., Mattauer, M., Bodeur, Y., Séguret, M., Puech, J. P., Mattei, J., 1978. Carte Géologique De La France Au 1/50.000. Feuille De St Martin De Londres N 963. BRGM. Orléans.

Pitra, P., Poujol, M., Driessche, J.V.D., Poilvet, J.-C., Paquette, J.-L., 2012. Early Permian extensional shearing of an Ordovician granite: The Saint-Eutrope "C/S-like" orthogneiss (Montagne Noire, French Massif Central). C. R. Geosci. 344, 377–384. https://doi.org/10.1016/j.crte.2012.06.002.

Pitra, P., Poujol, M., van Den Driessche, J., Bretagne, E., Lotout, C., Cogné, N., 2022. Late Variscan (315 Ma) subduction or deceptive zircon REE patterns and U-Pb dates from migmatite-hosted eclogites? (Montagne Noire, France). J. Metam. Geol. 40, 39–65. https://doi.org/10.1111/jmg.12609.

Poilvet, J.-C., Poujol, M., Pitra, P., Driessche, J.V.D., Paquette, J.-L., 2011. The Montalet granite, Montagne Noire, France: An Early Permian syn-extensional pluton as evidenced by new U-Th-Pb data on zircon and monazite. C. R. Geosci. 343, 454–461. https://doi.org/10.1016/j.crte.2011.06.002.

Poujol, M., Pitra, P., Driessche, J.V.D., Tartèse, R., Ruffet, G., Paquette, J.-L., Poilvet, J.-C., 2017. Two-stage partial melting during the Variscan extensional tectonics (Montagne Noire, France). Int. J. Earth Sci. 106, 477–500. https://doi.org/10.1007/s00531-016-1369-1.

Putzolu, F., Piccolo Papa, A., Mondillo, N., Boni, M., Balassone, G., Mormone, A., 2018. Geochemical Characterization of Bauxite Deposits from the Abruzzi Mining District (Italy). Minerals 8, 298. https://doi.org/10.3390/min8070298.

Reimann, C., Filzmoser, P., Garrett, R., Dutter, R., 2011. Statistical data analysis explained: applied environmental statistics with R. Wiley, Chichester, United Kingdom, 343 p.

Reinhardt, N., Proenza, A.J., Villanova-de-Benavent, C., Aiglsperger, T., Bover-Arnal, T., Torró, L., Salas, R., Dziggel, A., 2018. Geochemistry and Mineralogy of Rare Earth Elements (REE) in Bauxitic Ores of the Catalan Coastal Range. NE Spain. Minerals 2018 (8), 562. https://doi.org/10.3390/min8120562.

Ricordel-Prognon, C., Lagroix, F., Moreau, M.-G., Thiry, M., 2010. Lateritic paleoweathering profiles in French Massif Central: Paleomagnetic datings. J. Geophys. Res. 115, B10104. https://doi.org/10.1029/2010JB007419.

Roger, F., Teyssier, C., Respaut, J.-P., Rey, P.F., Jolivet, M., Whitney, D.L., Paquette, J.-L., Brunel, M., 2015. Timing of formation and exhumation of the Montagne Noire double dome, French Massif Central. Tectonophysics 640–641, 53–69. https://doi.org/10.1016/j.tecto.2014.12.002.

Rousset, C., 1969. Le bombement varois, relation entre la bauxitisation au Crétacé moyen en Provence et l'évolution originale de la région en regime karstique. C. R. Acad. Sci. Paris 268, 2331–2334.

Rousset, C., 1968. Contribution à l'étude des karsts du Sed-Est de la France: altérations morphologiques et minerals. Ph.D. thesis, University of Marseille. 533 p.

Schettino, A., Turco, E., 2011. Tectonic history of the western Tethys since the Late Triassic. Geol. Soc. Am. Bull. 123, 89–105. https://doi.org/10.1130/B30064.1.

Schmid, S.M., Fügenschuh, B., Kissling, E., Schuster, R., 2004. Tectonic map and overall architecture of the Alpine orogen. Eclogae Geol. Helv. 97 (1), 93–117. https://doi.org/10.1007/s00015-004-1113-x.

Séranne, M., 1999. The Gulf of Lion continental margin (NW Mediterranean) revisited by IBS: an overview. In: Durand, B., Jolivet, L., Horváth, F.,Séranne, M. (Eds.) The Mediterranean Basins: Tertiary extension within the Alpine Orogen. Geol. Soc. Sp. 156, 15–36.

Shamanian, G.H., Hattori, K., 2021. Neoproterozoic evolution of northern Gondwana recorded in detrital zircon grains from the Gheshlagh bauxite deposit, Alborz Mountains, Iran Block. Gondwana Res. 93, 184–196. https://doi.org/10.1016/j.gr.2020.12.033.

Simon-Coinçon, R., Thiry, M., Schmitt, J.-M., 1997. Variety and relationship of weathering features along the early Tertiary paleosurface in the southwestern French Massif Central and the nearby Aquitaine Basin. Palaeogeogr. Palaeocl. Palaeoecol. 129, 51–79. https://doi.org/10.1016/S0031-0182(96)00122-8.

Sláma, J., Košler, J., Condon, D.J., Crowley, J.L., Gerdes, A., Hanchar, J.M., Horstwood, M.S.A., Morris, G.A., Nasdala, L., Norberg, N., Schaltegger, U., Schoene, B., Tubrett, M.N., Whitehouse, M.J., 2008. Plešovice zircon — a new natural reference material for U-Pb and Hf isotopic microanalysis. Chem. Geol. 249, 1–35.

Stampfli, G.M., Borel, G.D., 2002. A plate tectonic model for the Paleozoic and Mesozoic constrained by dynamic plate boundaries and restored synthetic oceanic isochrons. Earth Planet. Sci. Lett. 196 (1), 17–33. https://doi.org/10.1016/S0012-821X(01)00588-X.

Stephan, T., Kroner, U., Romer, R.L., 2019. The pre-orogenic detrital zircon record of the Peri-Gondwanan crust. Geol. Mag. 156, 281–307. https://doi.org/10.1017/s0016756818000031.

Stevard, A., 1863. Sur un nouveau mineral d'aluminium. Rev Univ. Mines, Paris 14, 387–388.

Tardy, Y., Nahon, D., 1985. Geochemistry of laterites, stability of A-goethite, Al-hematite, and Fe3+-kaolinite in bauxites and ferricretes: an approach to the mechanism of concretion formation. Am. J. Sci. 285, 865–903.

Tavani, S., Bertok, C., Granado, P., Piana, F., Salas, R., Vigna, B., Munoz, J.A., 2018. The Iberia-Eurasia plate boundary east of the Pyrenees. Earth Sci. Rev. 187, 314–337. https://doi.org/10.1016/j.earscirev.2018.10.008.

Taylor, G., Eggleton, R.A., 2008. Genesis of pisoliths and of the Weipa Bauxite deposit, northern Australia. Aust. J. Earth Sci. 55 (S1), S87–S103.

Thiry, M., Quesnel, F., Yans, J., Wyns, R., Vergari, A., Theveniaut, H., Simon-Coinçon, R., Ricordel, C., Moreau, M.G., Giot, D., Dupuis, C., Bruxelles, L., Barbarand, J., Baele, J.-M., 2006. Continental France and Belgium during the Early Cretaceous: Paleoweatherings and paleolandforms. B. Soc. Geol. Fr. 177 (3), 155–175.

Torró, L., Proenza, J.A., Aiglsperger, T., Bover-Arnal, T., Villanova-de-Benavent, C., Rodríguez-García, D., Ramírez, A., Rodríguez, J., Mosquea, L.A., Salas, R., 2017. Geological, geochemical and mineralogical characteristics of REE-bearing Las Mercedes bauxite deposit. Dominican Republic. Ore Geol. Rev. 89, 114–131. https://doi.org/10.1016/j.oregeorev.2017.06.017.

Trap, P., Roger, F., Cenki-Tok, B., Paquette, J.-L., 2017. Timing and duration of partial melting and magmatism in the Variscan Montagne Noire gneiss dome (French Massif Central). Int. J. Earth Sci. 106, 453–476. https://doi.org/10.1007/s00531-016-1417-x.

Tugend, J., Manatschal, G., Kusznir, N.J., 2015. Spatial and temporal evolution of hyperextended rift systems: implication for the nature, kinematics, and timing of the Iberian-European plate boundary. Geology 43 (1), 15–18. https://doi.org/10.1130/G36072.1.

Valeton, I., Klint, W., 1962. Petrographie der bauxite von Mazaugues/Sudfrankreich. Geologisches Staatsinstitut, Hamburg 13, Von-Melle-Park 11 p.

van Hinsbergen, D.J.J., Torsvik, T.H., Schmid, S.M., Maţenco, L.C., Maffione, M., Vissers, R.L.M., Gürer, D., Spakman, W., 2020. Orogenic architecture of the Mediterranean region and kinematic reconstruction of its tectonic evolution since the Triassic. Gondw. Res. 81, 79–229. https://doi.org/10.1016/j.gr.2019.07.009.

Vermeesch, P., 2013. Multi-sample comparison of detrital age distributions. Chem. Geol. 341, 140–146. https://doi.org/10.1016/j.chemgeo.2013.01.010.

Wang, R., Wang, Q., Kirkland, C.L., Ramanaidou, E., Deng. J., 2023. Provenance shifts in bauxitic clay from Zibo, North China Craton, links tectonics and climate to environmental perturbation. Geosphere 20(1), 198–213. https:// doi .org / 10.1130/GES02656.1.

Wang, R., Wang, Q., Huang, Y., Yang, S., Liu, X., Zhou, Q., 2018. Combined tectonic and paleogeographic controls on the genesis of bauxite in the Early Carboniferous to Permian Central Yangtze Island. Ore Geol. Rev. 101, 468–480. https://doi.org/10.1016/j.oregeorev.2018.07.013.

Weissel, J.K., Karner, G.D., 1989. Flexural uplift of rift flanks due to mechanical unloading of the lithosphere during extension. J. Geophys. Res.-Sol. Ea. 94 (B10), 13919–13950.

Whitney, D.L., Roger, F., Teyssier, C., Rey, P.F., Respaut, J.-P., 2015. Syn-collapse eclogite metamorphism and exhumation of deep crust in a migmatite dome: The P-T–t record of the youngest Variscan eclogite (Montagne Noire, French Massif Central). Earth Planet. Sci. Lett. 430, 224–234. https://doi.org/10.1016/j.epsl.2015.08.026.

Whitney, D.L., Hamelin, C., Teyssier, C., Raia, N.H., Korchinski, M.S., Seaton, N.C.A., Bagley, B.C., Handt, A., Roger, F., Rey, P.F., 2020. Deep crustal source of gneiss dome revealed by eclogite in migmatite (Montagne Noire, French Massif Central). J. Metam. Geol. 38, 297–327. https://doi.org/10.1111/jmg.12523.

Wiedenbeck, M., Allé, P., Corfu, F., Griffin, W.L., Meier, M., Oberli, F., Quadt, A.V., Roddick, J.C., Spiegel, W., 1995. Three natural zircon standards for U-Th-Pb, Lu-Hf, trace element and REE analyses. Geostand. Geoanal. Res. 19, 1–23.

Yang, S., Wang, Q., Liu, X., Kana, Z., Santosh, M., Deng, J., 2022. Global spatio-temporal variations and metallogenic diversity of karst bauxites and their tectonic, paleogeographic and paleoclimatic relationship with the Tethyan realm evolution. Earth Sci. Rev. 233, 104144. https://doi.org/10.1016/j.earscirev.2022.104184.

Yu, W., Oggiano, G., Mongelli, G., Zhou, J., Buccione, R., Xu, L., Mameli, P., Du, Y., 2023. U-Pb detrital zircon ages and Hf isotope from Sardinia and Adria Cretaceous bauxite (Italy): constraints on the Alpine Tethys paleogeography and tectonic evolution. Ore Geol. Rev. 153, 105272. https://doi.org/10.1016/j.oregeorev.2022.105272.

Yuste, A., Bauluz, B., Mayayo, M.J., 2014. Genesis and mineral transformations in Lower Cretaceous karst bauxites (NE Spain): climatic influence and superimposed processes. Geol. J., 50. November/december 2015, 839–857. https://doi.org/10.1002/gj.2604.

Zhang, L., Park, C., Wang, G., Wu, C., Santosh, M., Chung, D., Song, Y., 2017. Phase transformation processes in karst-type bauxite deposit from Yunnan area, China. Ore Geol. Rev. 89, 407–420. https://doi.org/10.1016/j.oregeorev.2017.06.026.

Zhang, L., Wang, G., Park, C., Santosh, M., Zhang, J.Q., Han, F., Kwon, S.-T., Zhao, Z., Li, D., Zhou, J., Tang, Y., Song, Y., 2019. Tectonic evolution of north-eastern Tethyan Himalaya: evidence from U-Pb geochronology and Hf isotopic geochemistry of detrital zircons. Geol. J. 55 (5), 3694–3715. https://doi.org/10.1002/gj.3617.